Platinum Complexes of a Borane-Appended Analogue of 1,1'-Bis(diphenylphosphino)ferrocene: Flexible Borane Coordination Modes and *In-Situ* Vinylborane Formation

Bradley E. Cowie and David J. H. Emslie*[a]

Abstract: A bis(phosphine)-borane ambiphilic ligand, [Fe(η^5-$C_5H_4PPh_2$)(η^5-$C_5H_4P^tBu${$C_6H_4(BPh_2)$-*ortho*})] (**FcPPB**), in which the borane occupies a terminal position, was prepared. Reaction of FcPPB with tris(norbornene)platinum(0) provided [Pt(FcPPB)] (**1**) in which the arylborane is η^3*BCC*-coordinated. Subsequent reaction with CO and CNXyl afforded [PtL(FcPPB)] {L = CO (**2**) and CNXyl (**3**)} featuring η^2*BC*- and η^1*B*-arylborane coordination modes, respectively. Reaction of **1** or **2** with H_2 yielded [PtH(μ-H)(FcPPB)] in which the borane is bound to a hydride ligand on platinum. Addition of PhC_2H to [Pt(FcPPB)] afforded [Pt(C_2Ph)(μ-H)(FcPPB)] (**5**), which rapidly converted to [Pt(FcPPB')] (**6**; FcPPB' = [Fe(η^5-$C_5H_4PPh_2$)(η^5-$C_5H_4P^tBu${C_6H_4(BPh–CPh=CHPh-*Z*)-*ortho*}]) in which the newly formed vinylborane is η^3*BCC*-coordinated. Unlike arylborane complex **1**, vinylborane complex **6** does not react with CO, CNXyl, H_2 or HC_2Ph at room temperature.

Introduction

Monodentate σ-donating ligands, with or without the possibility for π-donation or π-acceptance, are ubiquitous in transition metal chemistry, either as neutral donors (e.g. NH_3, PR_3, CO; L-type ligands) or anionic donors (e.g. Cl^-, NR_2^-, H^-; X-type ligands). By contrast, σ-acceptor ligands (e.g. group 13 Lewis acids), designated Z-type ligands, are rare, and complexes bearing σ-acceptor ligands have the potential to promote unique reactivity given their: (a) high *trans* influence,[1,2] (b) ability to reduce by two units the number of d-electrons in a complex (i.e. the number of electrons in the frontier orbitals) without changing the overall electron count, (c) propensity to yield compounds with unusual coordination geometries,[3,4] (d) ability to stabilize complexes in a range of oxidation states by modulating the amount of electron density at the metal centre through metal-Lewis acid interactions of varying strength,[5,6] and (e) potential to engage in Lewis acid–substrate or metal–(co-ligand)–Lewis acid bridging interactions,[7,8] (f) potential to form zwitterions through anionic ligand abstraction, in some cases resulting in substituent exchange between boron and the metal centre,[9-12] and (g) potential to promote 1,1-insertion reactions.[13] They are therefore of emerging interest as supporting ligands in catalysis.[12,14-16]

While η^1*B*-coordinated complexes of simple borane ligands have proven elusive, the use of ambiphilic ligands, which contain both Lewis basic donors and a Lewis acidic σ-acceptor within the same ligand framework, has provided access to a range of supported transition metal–borane complexes. This concept was first demonstrated in 1999 when Hill *et al.* reported the reaction of Na[B(mt)$_3$] with [RuCl(R)(CO)(PPh_3)$_2$] {R = CH=CHCPh_2OH, CH=CH_2, CH=CH(*p*-MeC_6H_4) or Ph} to afford [Ru{B(mt)$_3$}(CO)(PPh_3)] (mt = 2-sulfanyl-1-methylimidazole); the borane in this complex was generated *in situ* by RH elimination from initially formed [Ru(R)(CO)(PPh_3){HB(mt)$_3$}].[17] Although effective, *in-situ* ambiphilic ligand generation lacks some generality, and has primarily been observed for tris(pyrazolyl)hydroborate and related facially capping hydroborate anions.

In 2006, Bourissou reported the synthesis of [AuCl{(^{i}Pr$_2$P)$C_6H_4BR_2$] (BR_2 = BCy_2, BFlu; Flu = fluorenyl) which features η^1*B*-coordination; this complex was prepared via the reaction of isolated (^{i}Pr$_2$P)$C_6H_4BR_2$ (BR_2 = BCy_2, BFlu) with [AuCl(SMe_2)].[7] Related [*o*-(R_2P)C_6H_4]$_2$BPh (R = ^{i}Pr, Ph) and [*o*-(^{i}Pr$_2$P)C_6H_4)]$_3$B ligands were subsequently prepared, and deployed in the preparation of Rh, Ni, Pd, Pt, Cu, Ag, and Au complexes, all of which exhibit η^1*B*-borane coordination to the metal centre.[4,7,18] The chemistry of these ligands and closely related derivatives has recently been expanded by Peters,[1,6,12,14,15,19] Nakazawa,[20,21] Stephan,[22] Echavarren,[23] and Bourissou.[16,24]

Also in 2006, we reported an isolable ambiphilic ligand, TXPB (2,7-di-*tert*-butyl-5-diphenylboryl-4-diphenylphosphino-9,9-dimethylthioxanthene), which features a phosphine donor and a borane acceptor anchored to a rigid thioxanthene backbone. In contrast to the aforementioned phosphine-borane ligands, TXPB did not yield η^1*B*-borane complexes. Instead, [Ni(TXPB)], [Pd(TXPB)] and [(TXPB)Rh(μ-CO)$_2$Fe(CO)Cp] were isolated featuring η^3*BCC*-arylborane coordination through boron and the *ipso*- and *ortho*-carbon atoms of a *B*-Phenyl ring.[25,26] Additionally, an η^2*BC*-arylborane complex, [Rh(CO)(TXPB)][PF_6], was isolated, in which rhodium is coordinated to boron and the *ipso*-carbon of a *B*-phenyl ring.[11]

The pendant borane in TXPB also proved to be available to participate in bonding with a range of co-ligands. For example, addition of TXPB to [Pd_2(dba)$_3$] (dba = *trans*,*trans*-dibenzylideneacetone) afforded [Pd(dba)(TXPB)] in which dba bridges between palladium and boron to generate a zwitterionic η^3-boratoxyallyl complex.[10] Furthermore, addition of isonitriles (RNC; R = *n*Bu, 2,6-dimethylphenyl, *para*-chlorophenyl) to [(TXPB)Rh(μ-CO)$_2$Fe(CO)Cp] provided [(TXPB)Rh(μ-CNR)(μ-CO)Fe(CO)Cp] complexes that feature a bridging borataaminocarbyne ligand.[27] Additionally, a range of Rh, Pd and Pt complexes with a halide bridging between the metal and the borane have been isolated.[11,28]

Although the TXPB ligand has been used to prepare a broad range of complexes, the central thioether donor is undesirably

[a] B. E. Cowie, Prof. D. J. H. Emslie
Department of Chemistry and Chemical Biology
McMaster University
1280 Main St. West, Hamilton, Ontario, L8S 4M1 (Canada)
E-mail: emslied@mcmaster.ca

Supporting information for this article is given via a link at the end of the document.

susceptible to displacement from the metal centre, especially in low-valent complexes. For example, addition of dvds (dvds = 1,3-divinyltetramethydisiloxane) to [Pd(TXPB)] formed [Pd(η^2:η^2-dvds)(κ^1*(P)*-TXPB)], in which Pd is removed from the central binding pocket of the ligand and TXPB acts as a monodentate phosphine.[26] Furthermore, addition of CO to [Pd(TXPB)] resulted in complete displacement of the TXPB ligand from the metal.

Herein we describe the syntheis of a new borane-containing ambiphilic ligand, FcPPB ([Fe(η^5-$C_5H_4PPh_2$)(η^5-$C_5H_4P^tBu\{C_6H_4(BPh_2)$-*ortho*$\}$)]; Scheme 1). This ligand features a bisphosphine donor set in place of the phosphine-thioether donor set of TXPB, thus improving the overall donor ability of the ligand. The ferrocene unit located between the two phosphorus donors in FcPPB provides increased coordinative flexibility relative to TXPB, while a rigid phenylene linker between the central donor and the borane is maintained in both TXPB and FcPPB. The borane in FcPPB is positioned at the extremity of the ligand framework, as is the case in TXPB; this is potentially desirable as a means to encourage the pendant borane to interact with substrates and co-ligands, with a view towards accessing cooperative reactivity involving both the metal and the borane. The FcPPB ligand can be considered a more electron donating and borane-substituted analogue of dppf [1,1'-bis(diphenylphosphino)ferrocene]; a wide bite-angle bis-phosphine ligand used extensively in late transition metal catalysis.[29] A range of FcPPB platinum complexes are described herein, each one featuring a different FcPPB coordination mode. Furthermore, reaction of phenylacetylene with platinum-coordinated FcPPB is described, transforming the arylborane (R_2B–Ph) group in FcPPB to a vinylborane (R_2B–CPh=CHPh).

Results and Discussion

The new PPB-donor/acceptor ligand, 1'-{(*ortho*-diphenylborylphenyl)-*tert*-butylphosphino}-1-diphenylphosphino ferrocene (FcPPB), was accessed in 7 steps, as shown in Scheme 1. Known [Fe(η^5-C_5H_4Br)(η^5-$C_5H_4PPh_2$)] was prepared as previously reported,[30] and the 2-bromophenyl-*tert*-butylphosphine moiety was incorporated into the ligand backbone by lithiation of the remaining bromide followed by quenching with (*o*-BrC_6H_4)^{t}BuPCl; (*o*-BrC_6H_4)^{t}BuPCl was prepared in three steps from commercially available 1,2-dibromobenzene and $ClP(NEt_2)_2$. Finally, lithiation of [Fe(η^5-$C_5H_4PPh_2$)\{η^5-$C_5H_4P^tBu(C_6H_4Br$-*o*$)$\}] followed by the addition of $BrBPh_2$ provided FcPPB. Intermediates (*o*-BrC_6H_4)^{t}BuPCl and [Fe(η^5-C_5H_4Br)(η^5-$C_5H_4PPh_2$)] were prepared on a 5-10 gram scale, and each of the final two steps proceeded in 70-80% yield, making FcPPB accessible in multi-gram quantities. FcPPB is chiral at phosphorus, and was used as a mixture of enantiomers.

X-ray quality crystals of FcPPB were grown by slow evaporation of a solution in CH_2Cl_2/hexanes at 298 K. The solid-state structure of FcPPB (Figure 1) revealed adduct formation between the *tert*-butyl substituted phosphorus donor, P(2), and the borane; the B–P(2) bond distance in FcPPB is 2.146(2) Å, the P(2)–C(27)–C(28) and B–C(28)–C(27) angles are 98.4(1)° and 106.6(1)°, respectively (rather than 120°) and the sum of the C–B–C angles is 347.5(2)° (rather than 360°). The B–P(2) bond distance in FcPPB is very similar to the B–P distance in [*o*-(^{i}Pr$_2$P)C_6H_4]$_3$B [B–P = 2.150(3) Å].[31] The ^{11}B NMR signal for FcPPB in [D_6]benzene is 17 ppm, which is at much lower frequency than expected for a free triarylborane, indicating that phosphine-borane adduct formation persists in solution.[32] A shift in the ^{31}P NMR signal for the $C_5H_4P(^tBu)$Ar moiety from 4.9 ppm in [Fe(η^5-$C_5H_4PPh_2$)\{η^5-$C_5H_4P^tBu(C_6H_4Br$-*o*$)$\}] to 19.7 ppm in FcPPB further supports this interpretation.

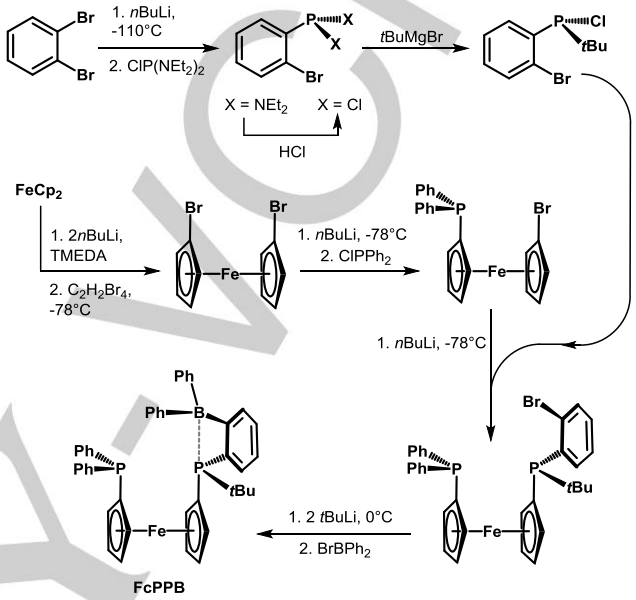

Scheme 1. Synthesis of FcPPB.

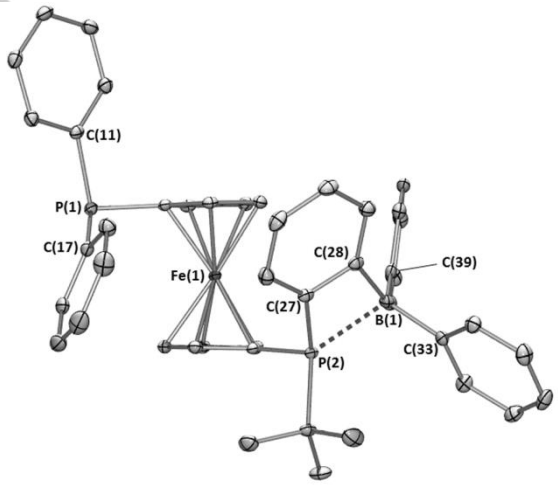

Figure 1. Solid-state structure of FcPPB with ellipsoids drawn at 50% probability. Hydrogen atoms have been omitted for clarity. Selected bond lengths [Å] and angles [°]: P(2)–B(1), 2.146(2); C(28)–B(1)–C(33), 115.2(2); C(28)–B(1)–C(39), 118.2(1); C(33)–B(1)–C(39), 114.1(1); C(28)–B(1)–P(2), 79.1(1); (C27)–P(2)–B(1), 75.73(8).

Reaction of FcPPB with [Pt(nb)$_3$] (nb = norbornene) yielded a pale yellow solid identified as [Pt(FcPPB)] (**1**) by multinuclear NMR spectroscopy, combustion elemental analysis, and X-ray crystallography. The ^{11}B NMR chemical shift of 21 ppm is

indicative of 4-coordinate boron, and although the *B*-phenyl groups give rise to just three signals in the ^{1}H NMR spectrum at 25 and –90 °C, single crystal X-ray diffraction revealed η^3*BCC*-arylborane coordination to platinum in the solid state (Figure 2), with Pt–B, Pt–C_{ipso} and Pt–C_{ortho} distances of 2.292(3), 2.225(3) and 2.329(3) Å. Boron is only slightly pyramidalized with the sum of the C–B–C angles equal to 354.3(5)°, and the geometry at platinum is pseudo square planar, analogous to that in [Pt(η^3-allyl)$(PPh_3)_2$]$^+$.[33] The M–B, M–C_{ipso} and M–C_{ortho} bond distances in previously reported η^3-arylborane complexes of group 10 metals are 2.320(5), 2.198(4) and 2.325(4) Å, respectively in [Pd(TXPB)], 2.297(4) Å, 2.019(3) and 2.081(3) Å in [Ni(TXPB)],[26] and 2.1543(9), 2.0751(8) and 2.1616(8) Å in [Ni(^{Mes}DPB^{Ph})] [^{Mes}DPB^{Ph} = Mes*B*{(*o*-Ph_2*P*)C_6H_4}$_2$; Mes = 2,4,6-trimethylphenyl].[14] Although the M–B, M–C_{ortho} and M–C_{ipso} distances in **1** and [Pd(TXPB)] are equal within error, the ^{11}B NMR chemical shift for **1** is significantly lower in frequency than those for [Pd(TXPB)] and [Ni(TXPB)] (20 versus 31 and 30 ppm, respectively), consistent with (a) increased electron donation from the metal to the borane in **1** due to the increased donor ability of the central phosphine donor of FcPPB relative to the thioether group in TXPB,[26] and (b) the increased basicity of Pt relative to Pd and Ni.[18a]

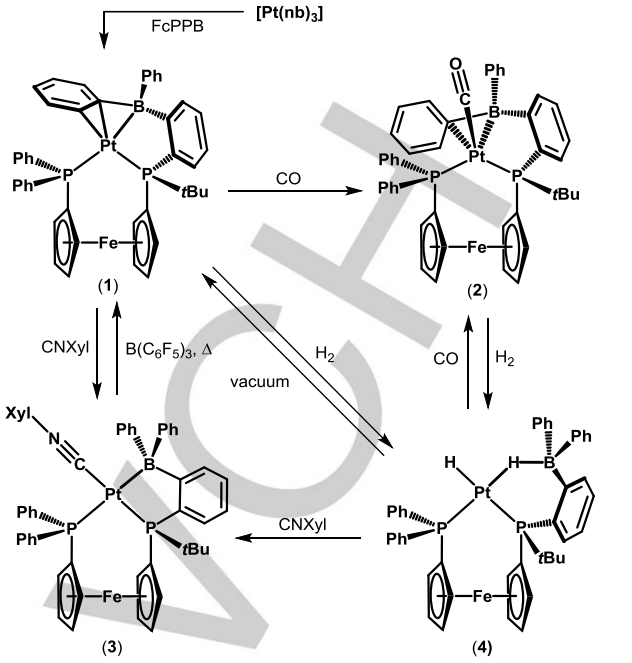

Scheme 2. Synthesis of [Pt(FcPPB)] (**1**), [Pt(CO)(FcPPB)] (**2**), [Pt(CNXyl)(FcPPB)] (**3**) and [PtH(μ-H)(FcPPB)] (**4**).

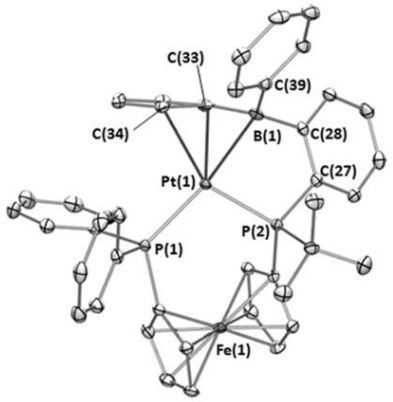

Figure 2. Solid-state structure of **1**·CH_2Cl_2 with ellipsoids drawn at 50% probability. Hydrogen atoms and lattice solvent have been omitted for clarity. Selected bond lengths [Å] and angles [°] for **1**·CH_2Cl_2: Pt(1)–B(1), 2.292(3); Pt(1)–C(33), 2.225(3); Pt(1)–C(34), 2.329(3); Pt(1)–P(1), 2.3014(8); Pt(1)–P(2), 2.2342(9); B(1)–C(33), 1.551(5); C(28)–B(1)–C(33), 118.4(3); C(28)–B(1)–C(39), 117.6(3); C(33)–B(1)–C(39), 118.0(3); P(1)–Pt(1)–B(1), 171.1(1); P(2)–Pt(1)–C(34), 148.32(7).

Reaction of **1** with CO or CNXyl (Xyl = 2,6-dimethylphenyl) afforded [Pt(CO)(FcPPB)] (**2**) and [Pt(CNXyl)(FcPPB)] (**3**) (Scheme 2) with ν(CO) and ν(CN) of 1982 and 2128 cm^{-1} in CH_2Cl_2, respectively, consistent with terminally bound carbonyl and isonitrile ligands.[34] Compound **2** did not react with $B(C_6F_5)_3$, whereas compound **3** reacted over days when heated to 90 °C to re-form complex **1**. For **2** and **3**, as in complex **1**, each of the *B*-phenyl groups gave rise to just three signals in the ^{1}H NMR spectrum between 25 and –90 °C. The ^{11}B chemical shifts for **2** and **3** are 19 and 10 ppm, consistent with 4-coordinate boron.

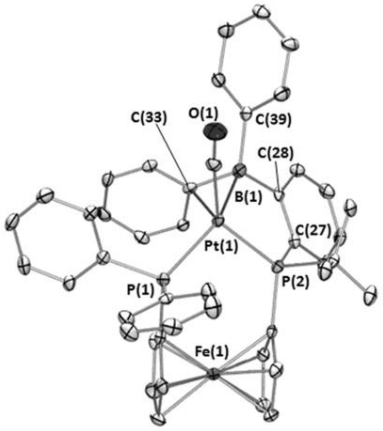

Figure 3. Solid-state structure of **2**·$2CH_2Cl_2$ with ellipsoids drawn at 50% probability. Hydrogen atoms and lattice solvent have been omitted for clarity. Selected bond lengths [Å] and angles [°] for **2**·$2CH_2Cl_2$: Pt(1)–B(1), 2.319(5); Pt(1)–C(33), 2.490(5); Pt(1)–P(1), 2.369(1); Pt(1)–P(2), 2.284(1); B(1)–C(33), 1.597(7); C(28)–B(1)–C(33), 114.9(4); C(28)–B(1)–C(39), 113.4(4); C(33)–B(1)–C(39), 116.7(4); P(2)–Pt(1)–B(1) = 82.4(1); P(1)–Pt(1)–B(1) = 146.2(1)°; B(1)–Pt(1)–C(45) = 88.9(2)°.

Single crystals of **2** were obtained from CH_2Cl_2/hexane at –30 °C, and X-ray diffraction revealed that the η^3*BCC*-arylborane coordination mode in **1** has been converted to an η^2*BC*-coordination mode in **2** (Figure 3). The two phosphorus donors, CO and C_{ipso} [CO = C(45); C_{ipso} = C(33)] adopt a distorted tetrahedral arrangement around platinum with a 73.2° angle between the P(1)–Pt–P(2) plane and the C(33)–Pt–C(45) plane [the angle between the the P(1)–Pt–P(2) plane and the B–Pt–C(45) plane is 50.4°]. The P(1)–Pt–P(2), P(X)–Pt-C(45) (X = 1 or 2), P(2)–Pt–C(33) and C(33)–Pt–C(45) angles are all between 100 and 107°, whereas P(2)–Pt–C(45) is 134.0(2)°. The Pt–B and Pt–C_{ipso} distances are 2.319(5) and 2.490(5) Å, respectively, and boron is significantly pyramidalized with the sum of the C–

B–C angles equal to 345.0(7)°. Related Group 10 complexes featuring bisphosphine and η^2*BC*-arylborane coordination include [Ni(THF)(^{Ph}DPB^{Ph})] [^{R}DPB^{Ph}= Ph*B*{(*o*-R$_2$*P*)C$_6$H$_4$}$_2$; Ni–B: 2.124(2) Å; Ni–C$_{ipso}$: 2.176(2) Å; Σ(CBC): 352.1(3)°],[14] and [Ni(N$_2$)(^{iPr}DPB^{Ph})] [Ni–B: 2.201(2)/2.181(2) Å; Ni–C$_{ipso}$: 2.170(2)/2.149(2) Å; Σ(CBC): 353°; ^{11}B NMR 20 ppm].[1] Similarly to **2**, the two phosphorus donors, C$_{ipso}$ and the remaining co-ligand (THF and N$_2$, respectively), in the above nickel complexes exhibit distorted tetrahedral geometry. While the M–B bond distances in the above two literature complexes are in good agreement with **2**, taking into account the smaller covalent radius of Ni (1.24 Å) versus Pt (1.36 Å),[35] the M–C$_{ipso}$ bond length in **2** is significantly longer than those in the nickel complexes and boron is more pyramidal, indicating that arylborane–platinum coordination in **2** consists of a strong Pt–B and a weak Pt–C$_{ipso}$ bonding interaction. The Pt–C$_{ipso}$ distance in **2** is also significantly longer than either the Pt–C$_{ipso}$ or the Pt–C$_{ortho}$ distance in **1**, despite comparable Pt–B bond lengths.

X-ray quality crystals of complex **3** were grown by slow diffusion of hexanes into a solution of **3** in CH_2Cl_2 at –30°C; **3** crystallizes with two independent molecules within the unit cell. In contrast to **1** and **2**, the borane in compound **3** is η^1*B*-coordinated, and the geometry at platinum is distorted square planar with P(1)–Pt–B and P(2)–Pt–C(45) angles between 157.9(3) and 159.9(3)° (Figure 4). The Pt–B distance is 2.27(1)/2.28(1) Å and boron is almost tetrahedral with the sum of the C–B–C angles equal to 333(1)°. The P(1)–Pt–P(2) bite angle decreases from 108.53(3)° in **1**, to 104.56(4)° in **2**, and 100.7(1)/101.0(1)° in **3**, and the conformational flexibility of the bis(phosphino)ferrocene backbone is highlighted by the very different P(1)–Cent$^{1-5}$–Cent$^{6-10}$–P(2) [Cent^{x-y} = centroid of the cyclopentadienyl ring containing atoms C(x) to C(y)] dihedral angles: –30.4, –20.9 and 4.4/–0.9° in **1**, **2** and **3**, respectively.

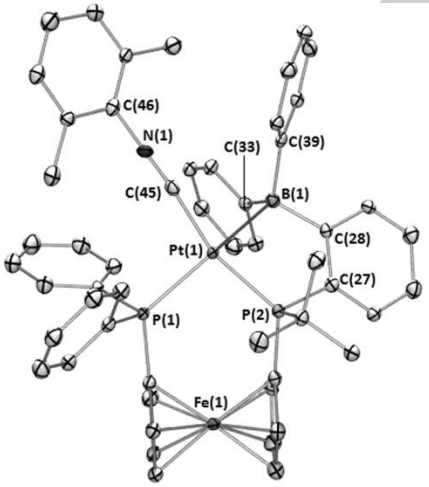

Figure 4. Solid-state structure of **3**·CH_2Cl_2 (only one of the two independent molecules in the unit cell is shown) with ellipsoids drawn at 50% probability. Hydrogen atoms and lattice solvent have been omitted for clarity. Selected bond lengths [Å] and angles [°] for **3**·CH_2Cl_2: Pt(1A)–B(1A), 2.273(12); Pt(1A)–C(45A), 1.952(10); Pt(1A)–P(1A), 2.381(2); Pt(1A)–P(2A), 2.268(3); C(45A)–N(1A), 1.170(12); C(28A)–B(1A)–C(33A), 109.1(8); C(28A)–B(1A)–C(39A), 109.9(8); C(33A)–B(1A)–C(39A), 114.0(8); C(45A)–N(1A)–C(46A), 176.2(9); Pt(1B)–B(1B), 2.281(11); Pt(1B)–C(45B), 1.978(9); Pt(1B)–P(1B), 2.369(2); Pt(1B)–P(2B), 2.271(2); C(45B)–N(1B), 1.147(11); C(28B)–B(1B)–C(33B), 108.4(8); C(28B)–B(1B)–C(39B), 111.5(8); C(33B)–B(1B)–C(39B), 113.4(8); C(45B)–N(1B)–C(46B), 175.1(9).

The ^{195}Pt resonances for **1**-**3** are located at –4934, –4422 and –4486 ppm, respectively. In the ^{31}P{^{1}H} NMR spectra of **1**-**3**, the C$_5$H$_4$*P*Ph$_2$ signal is observed at 28.5, 22.8 and 21.8 ppm, respectively [^1J(^{31}P-^{195}Pt) = 4183, 2343 and 1381 Hz], and the C$_5$H$_4$*P*(^{t}Bu)Ar group is observed at 50.8, 59.4 and 62.7 ppm, respectively [^1J(^{31}P-^{195}Pt) = 5651, 4884 and 4549 Hz]. The marked decrease in ^{31}P-^{195}Pt coupling constants for the C$_5$H$_4$*P*Ph$_2$ groups in **1**-**3** is likely due to the changes in arylborane coordination mode, with a greater *trans*-influence exerted by the η^1-borane, even though the P(1)–Pt–B bond angle more closely approaches 180° in compound **1** [P(1)–Pt–B = 171.0(1)° in **1**, 146.2(1)° in **2**, and 157.9(3)-159.9(3)° in **3**]. A marked increase in peak broadness is also observed in the ^{195}Pt{^{1}H} NMR spectra for **1**-**3**, with $\omega_{1/2}$ increasing from 95 to 125 to 300 Hz, respectively, arguably due to stronger bonding of platinum to quadrupolar boron in the order **1** < **2** < **3**.

Reaction of **1** with H_2 (1 atm) afforded [PtH(μ-H)(FcPPB)] (**4**), which is also generated by exposing carbonyl complex **3** to H_2 (1 atm). Compound **4** is stable under an atmosphere of H_2, but in solution under argon (slowly) or under vacuum (rapidly) it loses H_2 to re-form **1** (Scheme 2). Additionally, under an atmosphere of CO, **4** readily re-forms carbonyl complex **2**. The hydride signals for **4** are located at –2.76 and –5.19 ppm in the ^{1}H NMR spectrum. The lower frequency hydride signal is a sharp doublet of doublets and is *trans* to the C$_5$H$_4$*P*(^{t}Bu)Ar group, whereas the hydride ligand *trans* to the C$_5$H$_4$*P*Ph$_2$ group is a slightly broadened doublet of doublets, suggestive of a Pt–H–B bridging interaction; the ^{11}B NMR chemical shift of 5 ppm is consistent with this assignment.

Solid state IR spectroscopy of **4** was not possible due to the propensity of **4** to eliminate H_2 in the absence of a hydrogen atmosphere. However, in CH_2Cl_2 broad Pt–H and very broad Pt–H–B stretches were located at 2020 and 1822 cm^{-1}, respectively, in fair agreement with calculated values (2065 and 1868 cm^{-1}; ADF 2013.01, PBE, D3-BJ, TZ2P all-electron, ZORA). The Pt–H stretch for the terminally bound hydride is also in good agreement with platinum complexes *cis*-[PtH(Se^{t}Bu)(PPh$_3$)$_2$] [ν(Pt–H) = 2088 cm^{-1}][36] and [Pt$_2$H$_2$(μ-PR$_2$)$_2$(PEt$_3$)$_2$] [ν(Pt–H) = 2004 cm^{-1} (R = Ph); 2022 cm^{-1} (R = ^{t}Bu)].[37] Furthermore, [PtD(μ-D)(FcPPB)] (**4-D**) was prepared via reaction of [Pt(FcPPB)] with D_2, and the Pt–D stretching frequency (1478 cm^{-1}) was located by subtraction of the IR spectrum of **4** from that of **4-D**, due to overlap of these stretches with C=C and C–C stretches (the Pt–D–B stretch was not located).

Complete abstraction of the hydride ligand from platinum by boron does not occur in **4**, given that both hydride signals show coupling to ^{31}P and ^{195}Pt. However, a smaller ^{1}H-^{195}Pt coupling is observed for the bridging hydride (792 vs 905 Hz), consistent with a weakened Pt–H bond, despite its position *trans* to the lower *trans*-influence phosphine. The greater *trans*-influence of the terminal hydride is also evident from the ^{31}P{^{1}H} NMR spectrum of **4** which shows a larger ^1J(^{31}P-^{195}Pt) coupling of 3721 Hz for the C$_5$H$_4$*P*Ph$_2$ group (*trans* to the bridging hydride), relative to 2123 Hz for the C$_5$H$_4$*P*(^{t}Bu)Ar group, even though the latter is the better donor and has the higher ^1J(^{31}P-^{195}Pt) coupling in complexes **1**-**3**. The ^{195}Pt signal for **4** is a sharp doublet of doublets located at –4980 ppm.

Due to the propensity for **4** to revert back to **1** and H_2 in the absence of an H_2 atmosphere, we were unsuccessful in obtaining single crystals of **4**. However, DFT calculations on **4**

(ADF 2013.01, PBE, D3-BJ, TZ2P all-electron, ZORA) converged to a minimum with one bridging and one terminal hydride (Figure 5), consistent with the NMR data. The geometry at platinum is square planar, with Pt–P distances of 2.246 and 2.322 Å to the $C_5H_4PPh_2$ and $C_5H_4P(^tBu)Ar$ groups (the corresponding Mayer bond orders are 1.21 and 1.05), and Pt–H distances of 1.613 and 1.686 Å to the terminal and bridging hydride ligands, respectively. Boron is significantly pyramidalized [Σ(C–B–C): 338°], the Pt–B distance remains fairly short at 2.524 Å, and the B–H distance is 1.386 Å, which is longer than that observed for a free hydroborate anion (*e.g.* 1.10(2) Å in $[HC(SiMe_2OCH_2CH_2OCH_3)_3Na][Ph_3BH]$).[38] The Hirshfeld charges on Pt and B are 0.106 and –0.015, and the charges on the terminal and bridging hydrogen atoms are –0.093 and –0.048, indicating that **4** is not well represented as a zwitterion. The Pt–H(terminal), Pt–H(bridging), H–B and Pt–B Mayer bond orders are 0.81, 0.58, 0.39 and 0.23, respectively, suggesting that the borane in **4** interacts with both the bridging hydride and the metal centre. The H–B–C angles are 115.4, 109.3 and 92.4, with the acute angle to the phenyl *ipso* carbon, C(33), that is closest to *trans* to platinum across the H–B bond {Pt–H–B–C(33) torsion angle = 153°}; an acute (<100°) H–B–C angle was previously observed in the experimental and calculated structures of $[Rh(\mu\text{-}H)(PPh_3)(CO)_n\{PhB(C_6H_4PPh_2\text{-}ortho)_2\}]$ (n = 0 and 1).[21]

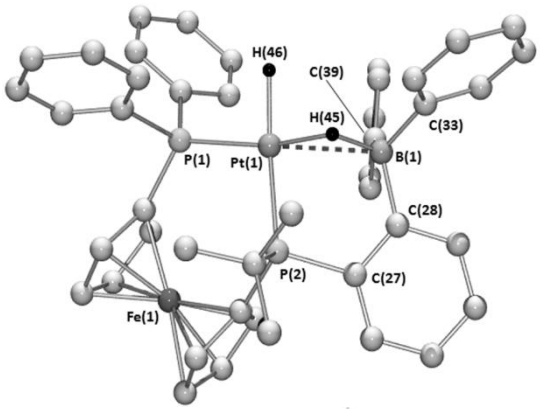

Figure 5. Calculated structure of **4** with most hydrogen atoms omitted for clarity.

The potential of **1** to hydrogenate alkenes and internal alkynes (C_2H_4, styrene, norbornene, cyclooctene, 1-octene, C_2Ph_2; 20 or 60 °C) was investigated, but significant catalytic activity was only observed for certain batches, and only in the absence of metallic mercury, indicative of heterogeneous catalysis by a small amount of elemental platinum. This contrasts the hydrogenation activity of the first row ambiphilic ligand complexes $[Fe(N_2)(^{iPr}TPB)]$ and $[Ni(^{iPr}DPB^{Mes})]$ reported recently by Peters *et al*.[12,14] Compound **1** does not react with any of the aforementioned alkenes or alkynes to an extent detectable by ^{1}H NMR spectroscopy. By contrast, reaction of **1** with PhC_2H resulted in rapid oxidative addition to provide $[Pt(C_2Ph)(\mu\text{-}H)(FcPPB)]$ (**5**), which isomerized within minutes to afford an η^3*BCC*-coordinated vinylborane complex, [Pt(FcPPB')] (**6A**; FcPPB' = $[Fe(\eta^5\text{-}C_5H_4PPh_2)(\eta^5\text{-}C_5H_4P^tBu\{C_6H_4(BPh\text{–}CPh{=}CHPh\text{-}Z)\text{-}ortho\}])$; after 5 minutes at room temperature, the reaction of **1** with PhC_2H contained a 1:1 mixture of **5** and **6A**.

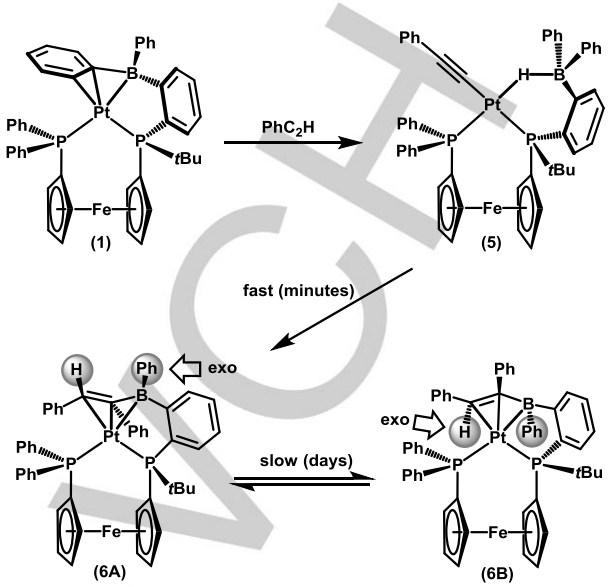

Scheme 3. Synthesis of $[Pt(C_2Ph)(\mu\text{-}H)(FcPPB)]$ (**5**) and [Pt(FcPPB')](**6A/6B**).

The hydride signal in **5** is located at –3.69 ppm in the ^{1}H NMR spectrum, with a $^1J(^1H\text{-}^{195}Pt)$ coupling of 760 Hz and $^2J(^1H\text{-}^{31}P)$ couplings of 115 and 12.0 Hz. An ^{11}B NMR chemical shift of 11 ppm indicates that the hydride ligand in **5** resides in a bridging position between platinum and boron, as was observed in **4**. The C≡C stretch for **5** was located at 2126 cm^{-1} in the IR spectrum,[39] which is very similar to that observed for *cis*-$[PtH(C_2C_6H_4Me\text{-}p)(PPh_3)_2]$ [ν(C≡C) = 2111 cm^{-1}].[39,40] Similar oxidative addition reactivity with HC_2Ph was reported recently for $[Fe(N_2)(^{iPr}TPB)]$, but in this case the resulting hydride is completely abstracted by the borane to afford zwitterionic $[Fe(C_2Ph)(^{iPr}TPB\text{-}H)]$ [ν(C≡C) = 2040 cm^{-1}; ν(B–H) = 2490 cm^{-1}].[12]

Complex **6A** is a vinylborane analogue of arylborane complex **1**, and both complexes feature an η^3*BCC*-coordination mode, almost identical ^{31}P NMR chemical shifts (50.3 and 27.6 for **6A**, 50.8 and 28.5 ppm for **1**) and similar ^{11}B NMR chemical shifts (24 and 21 ppm for **6A** and **1**, respectively). The platinum resonance is a sharp doublet of doublets located at –5117 ppm in the $^{195}Pt\{^1H\}$ NMR spectrum. In the ^{1}H NMR spectrum of **6A**, the BCPh=C*H*Ph signal is observed at 5.86 ppm as a doublet of doublets with platinum satelites. The vinyl carbon atoms in **6A** are located at 114.0 ppm (C^α, broad singlet) and 77.7 ppm [C^β, dd, $^2J(^{13}C\text{-}^{31}P)$ = 34, 4 Hz] in the ^{13}C NMR spectrum, demonstrating that η^3*BCC*-vinylborane coordination is maintained in solution, in contrast to η^3*BCC*-arylborane coordination in **1**. The $^1J(^{31}P\text{-}^{195}Pt)$ couplings for the $C_5H_4PPh_2$ groups in **6A** and **1** are similar (3937 Hz in **6A** vs 4183 Hz in **1**), whereas the $^1J(^{31}P\text{-}^{195}Pt)$ coupling for the $C_5H_4P(^tBu)Ar$ group is much smaller in **6A** than that in **1** (3695 Hz in **6A** vs 5651 Hz in **1**), suggesting that the vinyl group in **6A** exerts a substantially greater *trans*-influence than the phenyl group in **1**. The improved coordination ability of the *B*-vinyl group in **6A** relative to the *B*-

phenyl group in **1** is also reflected in the reactivity of **6A**, which does not react at room temperature with CO, CNXyl, H_2 or HC_2Ph.

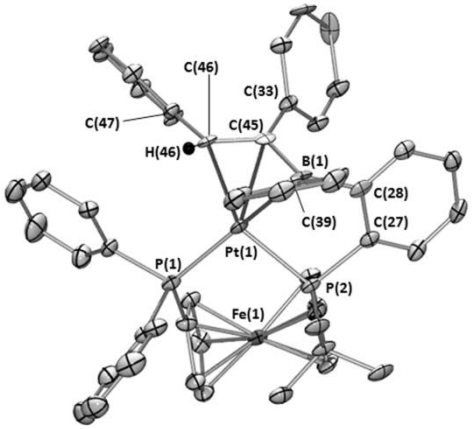

Figure 6. Solid-state structure of **6A**·$4C_6H_6$ with ellipsoids drawn at 50% probability. With the exception of H(46), all hydrogen atoms and lattice solvent have been omitted for clarity. Selected bond lengths [Å] and angles [°] for **6A**·$4C_6H_6$: Pt(1)–B(1), 2.303(6); Pt(1)–C(45), 2.184(5); Pt(1)–C(46), 2.194(5); Pt(1)–P(1), 2.295(2); Pt(1)–P(2), 2.278(1); B(1)–C(45), 1.546(8); C(45)–C(46), 1.447(8); C(28)–B(1)–C(45), 115.1(5); C(28)–B(1)–C(39), 117.4(5); C(39)–B(1)–C(45), 124.0(5); C(45)–C(46)–C(47), 123.2(5); C(33)–C(45)–C(46), 118.4(5); C(33)–C(45)–B(1), 121.5(5); C(45)–C(46)–H(46), 123(4); C(47)–C(46)–H(46), 109(4).

Single crystals of **6A** were obtained from a benzene/hexane solution cooled to –30 °C. In the solid state, complex **6A** adopts a distorted square planar geometry, with P(2)–Pt–C(46) and P(1)–Pt–B angles equal to 149.0(2) and 165.8(2)°, respectively (Figure 6). The Pt–B distance is 2.303(6) Å and the sum of the C–B–C angles is 356.5(9) °; these data are identical within error to those in **1**. By contrast, the Pt–C_α and Pt–C_β distances in **6A** [2.184(5) and 2.194(5) Å, respectively] are shorter than those in **1** by 0.041 and 0.135 Å. Even shorter Pt–C distances have previously been described for [Pt(P^tBu_3)(VB^{Ph})] [VB^{Ph} = (*E*)-PhHC=C(H)-*B*(C_6F_5)$_2$; two independent molecules in the unit cell; Pt–C_α = 2.126(4)/2.130(4) Å; Pt–C_β = 2.137(4)/2.155(4) Å; Pt–B = 2.273(5)/2.319(5) Å],[41] likely due to decreased steric hindrance and the greater Lewis acidity of the borane in VB^{Ph} (VB^{Ph} was shown to be an overall acceptor ligand in [Pt(P^tBu_3)(VB^{Ph})]). The B–C_α distance in **6A** is 1.546(8) Å, compared with 1.551(5) Å in **1** and 1.517(6)/1.519(7) Å in [Pt(P^tBu_3)(VB^{Ph})], but unfortunately, the standard deviation associated with the B–C_α bond in **6A** is too large to draw any conclusions regarding the extent of multiple bond character. The vinylic proton and the B–Ph ring [H(46) and C(39)] reside in the *exo* positions of the coordinated vinyl group and are located 0.419 and 0.922 Å above the B–C_α–C_β plane, respectively, whereas C_β–Ph and the phenylene linker of the backbone [C(47) and C(28)] reside in *endo* positions and bend towards the metal, placing them 0.565 and 0.086 Å below the B–C_α–C_β plane, respectively. Such distortions are typical of late transition metal–allyl complexes,[42] suggesting that the vinylborane in **6A** is more borataallyl-like than alkyl/borataalkene-like.[41]

Complex **6A** isomerizes over a period of 6 days at room temperature to an approximate 45:55 mixture of the original isomer and a new isomer, **6B**, giving rise to a new set of ^{31}P (55.7 and 23.3 ppm), ^{11}B (30 ppm) and ^{195}Pt (–4840 ppm) signals. As with **6A**, isomer **6B** features an η^3*BCC*-coordinated *Z*-(B–CPh=CHPh) group: (a) ^1H-^{13}C HSQC NMR confirmed that the vinyl proton is located in the β-position, (b) coupling between the ArPhB–CPh=C***H***Ph signal and the *o*-B***Ph*** signal in a selective 1D ^1H-^1H ROESY NMR experiment demonstrated that the ligand has a *Z*-arrangement of the phenyl substituents on the vinyl group (the vinyl C*H* proton in **6A** shows an analogous ROESY coupling), (c) the ^{11}B NMR chemical shift (30 ppm) confirmed coordination of boron to platinum, and (d) vinyl group ^1H-^{195}Pt, ^{13}C-^{195}Pt and ^{13}C-^{31}P coupling confirmed coordination of both the α- and β-carbon atoms of the vinyl ligand. The selective 1D ^1H-^1H ROESY NMR experiments also revealed that the vinyl proton and the *B*-phenyl groups in both **6A** and **6B** are positioned in the *exo* positions of the η^3*BCC*-coordinated vinylborane. Isomer **6B** is therefore related to **6A** by coordination of platinum to the opposite face of the vinylborane, with all of the regiochemistry of the *BCC* unit preserved (Scheme 3; isomer **6B** shows through-space coupling between the C*Ph*=CHPh group and the PC*Me*$_3$ group).

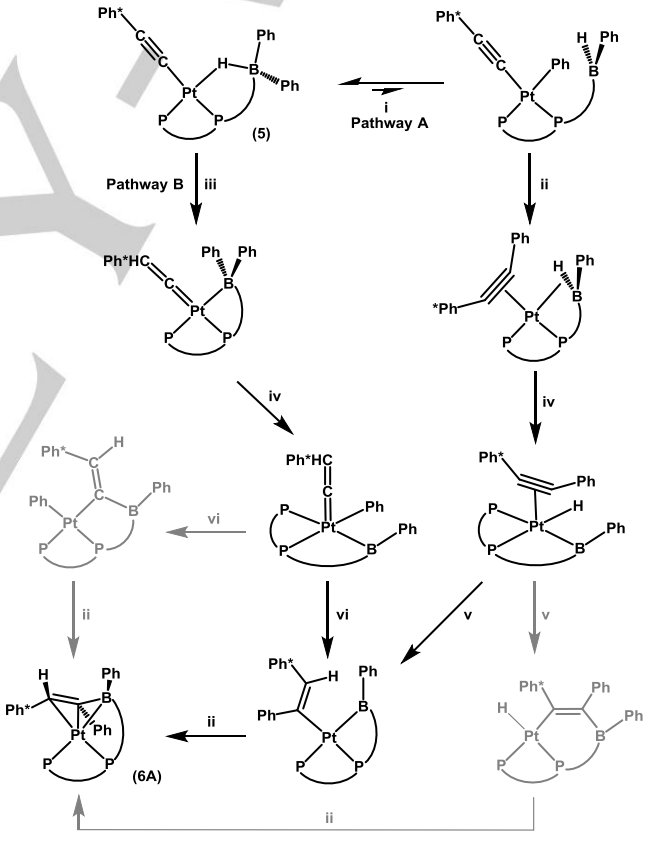

Scheme 4. Two Possible Reaction Pathways for the Formation of **6A.** Ph* indicates the phenyl group originating from phenylacetylene. Only one possible geometry and/or borane coordination mode is shown for proposed intermediates. Pathways relying on B–C bond-forming insertion reactions are shown in grey. Reactions: (i) hydride abstraction by the borane, followed by phenyl group transfer from boron to platinum, (ii) reductive elimination, (iii) alkynyl hydride–alkyne–vinylidene isomerization, (iv) oxidative addition, (v) 1,2-insertion, (vi) 1,1-insertion.

Two plausible reaction pathways for the formation of **6A** from **5** are shown in Scheme 4. Pathway A involves initial phenylacetylene C–H bond oxidative addition, exchange of a hydride on platinum with a phenyl group on boron, and C-C

bond-forming reductive elimination to generate a platinum(II) diphenylacetylene intermediate. Subsequent B–H bond oxidative addition, 1,2-insertion involving the C_2Ph_2 ligand and the newly-formed hydride ligand (or less likely the boryl ligand), and reductive elimination yields **6A**. By contrast, pathway B involves initial vinylidene formation, followed by sequential B–C bond oxidative addition, 1,1-insertion involving the vinylidene and a platinum phenyl or boryl group, and reductive elimination to form **6A**. A pathway involving migration of the vinylidene in [Pt(=C=CHPh)(FcPPB)] to a bridging position between boron and platinum was not considered viable given the electrophilic nature of the α-carbon of a vinylidene ligand.

Pathway A seems less likely given that [PtH(μ-H)(FcPPB)] does not eliminate benzene, which would be anticipated if the pendant borane is able to abstract a hydride and return a phenyl group to the metal centre. Additionally: (a) in the presence of a large excess of HC_2Ph, products consistent with C_2Ph_2 substitution by HC_2Ph and subsequent 1,2-insertion and reductive elimination are not observed, and (b) if free rotation or dissociation of C_2Ph_2 can occur, the phenyl group originating from boron could occupy either the α- or the β-position, and only the former is observed when the reaction is conducted with $HC_2(C_6D_5)$. However, with respect to the 1,1-insertion step in pathway B, it is of note that equivalent reactivity is not observed for [Pt(CO)(FcPPB)] (**2**) or [Pt(CNXyl)(FcPPB)] (**3**), which are analogues of proposed [Pt(=C=CHPh)(FcPPB)].

Conclusions

A wide bite-angle phosphine-phosphine-borane ambiphilic ligand, FcPPB {[Fe(η^5-$C_5H_4PPh_2$)(η^5-$C_5H_4P^tBu${$C_6H_4(BPh_2)$-*ortho*})]; Scheme 1}, has been prepared and utilized in the synthesis of a range of platinum complexes. This ligand is a borane-appended analogue of dppf {1,1'-bis(diphenylphosphino)ferrocene}, which is one of the most commonly employed bis-phosphine ligands in late transition metal catalysis. FcPPB is a superior ligand framework relative to our formerly employed phosphine-thioether-borane ambiphilic ligand, TXPB, given its overall improved donor ability and increased ligand backbone flexibility. The reactivity of [Pt(FcPPB)] with CO, CNXyl, H_2 and HC_2Ph highlights the coordinative flexibility of the triarylborane unit in FcPPB, providing reversible access to η^3*BCC*-, η^2*BC*- and η^1*B*-borane coordination modes, as well as Pt–H–BR_3 bridging interactions. This reactivity also demonstrates the ability of the FcPPB to promote oxidative addition reactivity, to maintain coordination of both donor groups in a range of oxidation states, and to stabilize varied coordination geometries at platinum, ranging from pseudo-square planar to pseudo-tetrahedral. Furthermore, the reaction of [Pt(FcPPB)] with HC_2Ph afforded [Pt(FcPPB')] (FcPPB' = [Fe(η^5-$C_5H_4PPh_2$)(η^5-$C_5H_4P^tBu$-{C_6H_4(BPh–CPh=CHPh-*Z*)-*ortho*}]) featuring the first vinylborane-containing ambiphilic ligand. This complex provides a unique opportunity for direct comparison of η^3*BCC*-arylborane and η^3*BCC*-vinylborane bonding and reactivity, and in the solid state, [Pt(FcPPB)] and [Pt(FcPPB')] are structurally similar. However, the latter features shorter Pt–C bonds, and whereas [Pt(FcPPB)] reacts with CO, CNXyl, H_2 and HC_2Ph at room temperature, [Pt(FcPPB')] does not, consistent with much tighter η^3*BCC*-coordination in the vinylborane complex. This suggests that arylborane-appended complexes are likely to be of more utility than vinylborane-appended complexes in the future development of cooperative catalysis. Overall, the application of ambiphilic ligand transition metal complexes for small molecule activation and catalysis is a rapidly emerging field, and the results described herein demonstrate initial reactivity of a new ambiphilic ligand featuring (a) a bis-phosphine unit that is well established in catalysis, and (b) a Lewis acid that occupies a terminal position in a donor-donor-acceptor array (as opposed to a central position in a donor-acceptor-donor array), potentially rendering it more accessible for substrate and co-ligand coordination. Future work will explore the utility of FcPPB in cooperative catalysis, and will compare the reactivity of FcPPB with analogues bearing alternative Lewis acidic groups; preparation of the required ligands is expected to be straightforward given that the Lewis acid is installed in the final step of the FcPPB ligand synthesis.

Experimental Section

An argon-filled MBraun UNIlab glove box equipped with a −30 °C freezer was employed for the manipulation and storage of the FcPPB ligand and its complexes, and reactions were performed on a double manifold high vacuum line using standard techniques.[43] A Fisher Scientific Ultrasonic FS-30 bath was used to sonicate reaction mixtures where indicated. Residual oxygen and moisture was removed from the argon stream by passage through an Oxisorb-W scrubber from Matheson Gas Products.

Anhydrous CH_2Cl_2 was purchased from Aldrich. Hexanes and toluene were initially dried and distilled at atmospheric pressure from CaH_2 and Na, respectively. Diethyl ether and tetrahydrofuran were initially dried and distilled at atmospheric pressure from Na/Ph_2CO. Unless otherwise noted, all proteo solvents were stored over an appropriate drying agent (toluene, benzene, diethyl ether, tetrahydrofuran = Na/Ph_2CO; hexanes = Na/Ph_2CO/tetra-glyme; CH_2Cl_2 = CaH_2) and introduced to reactions via vacuum transfer with condensation at −78 °C. Deuterated solvents (ACP Chemicals) were dried over CaH_2 (CD_2Cl_2) or Na/Ph_2CO (C_6D_6).

N,N,N',N'-tetramethylethane-1,2-diamine (TMEDA), 1,1,2,2-tetrabromoethane, 1,2-dibromobenzene, $ClPPh_2$, $HNEt_2$, 1,3,5,7-cyclooctatetraene, 1,5-cyclooctadiene, phenylacetylene, styrene, cyclooctene and 1-octene were purchased from Sigma-Aldrich and stored under argon following distillation from molecular sieves. $HC_2C_6D_5$ was purchased from CDN Isotopes and stored under argon. $BF_3{\cdot}Et_2O$ was purchased from Sigma-Aldrich and distilled from CaH_2 prior to use. Bicyclo[2.2.1]hept-2-ene and PCl_3 were purchased from Sigma-Aldrich and distilled *in vacuo* prior to use. ^{t}BuLi solution (1.7 M in pentane) was purchased from Sigma-Aldrich; ^{t}BuLi was isolated as a solid and stored under argon. Ferrocene, BBr_3, *n*BuLi solution (1.6 M in hexanes), ^{t}BuMgBr solution (2.0 M in Et_2O), HCl solution (4.0 M in dioxanes), CNXyl, lithium metal, magnesium turnings and diphenylacetylene were purchased from Sigma-Aldrich and either used as was or stored under argon. $SnPh_4$ was purchased from Eastman Organic Chemicals and used as was. C_6F_5Br was purchased from Oakwood Chemicals and distilled from molecular sieves prior to use. K_2PtCl_4 was purchased from Pressure Chemicals and used as was. CO of >99.0% purity was

purchased from Sigma-Aldrich. Argon and C_2H_4 of 99.999 % purity was purchased from Praxair. H_2 of 99.999 % purity was purchased from VitalAire. $BrBPh_2$ was prepared from $SnPh_4$ and BBr_3 according to the literature procedure.[44] $ClP(NEt_2)_2$, which was utilized to prepare $(o\text{-}BrC_6H_4)P(NEt_2)_2$, was prepared from PCl_3 and $HNEt_2$ according to the literature procedure.[45] $[Fe(\eta^5\text{-}C_5H_4Br)_2]$ was prepared from $[Fe(\eta^5\text{-}C_5H_4Li)_2(TMEDA)]$[46] according to the literature procedure.[47] $[Fe(\eta^5\text{-}C_5H_4Br)(\eta^5\text{-}C_5H_4PPh_2)]$ was prepared from $[Fe(\eta^5\text{-}C_5H_4Br)_2]$ according to the literature procedure.[30] $[Pt(nb)_3]$ was prepared from $[PtCl_2(COD)]$[48] according to the literature procedure.[49] $B(C_6F_5)_3$ was prepared from C_6F_5MgBr and $BF_3{\cdot}Et_2O$ according to the literature procedure.[50]

IR Spectra were recorded on a Thermo Scientific Nicolet 6700 FTIR spectrometer (reported stretches are strong unless otherwise noted). Combustion elemental analyses were performed on a Thermo EA1112 CHNS/O analyzer. High-resolution (HR) electron ionization (EI) mass spectrometry measurements were carried out on the Waters Micromass GCT instrument (quadrupole time-of-flight). A VWR Clinical 200 Large Capacity Centrifuge (with 28° fixed-angle rotors that hold 12 × 15 mL or 6 × 50 mL tubes) in combination with VWR high-performance polypropylene conical centrifuge tubes was used when required (inside the glovebox). NMR spectroscopy (^{1}H, ^{13}C{^{1}H}, ^{11}B, ^{31}P{^{1}H}, ^{195}Pt{^{1}H}, DEPT-135, uDEFT, COSY, ROESY, ^{1}H,^{13}C-HSQC, ^{1}H,^{13}C-HMBC, ^{1}H,^{31}P-HMBC) was performed on Bruker DRX-500 and AV-600 spectrometers. All ^{1}H NMR and ^{13}C NMR spectra were referenced relative to $SiMe_4$ through a resonance of the employed deuterated solvent or proteo impurity of the solvent; C_6D_6 (7.16 ppm) and CD_2Cl_2 (5.32 ppm) for ^{1}H NMR; C_6D_6 (128.0 ppm) and CD_2Cl_2 (54.0 ppm) for ^{13}C NMR. ^{11}B, ^{31}P{^{1}H} and ^{195}Pt{^{1}H} NMR spectra were referenced using an external standard of $BF_3(OEt_2)$ (0.0 ppm), 85% H_3PO_4 in D_2O (0.0 ppm) and 1.2 M $Na_2[PtCl_6]$ in D_2O (0.0 ppm), respectively. Temperature calibration was performed using a d_4-methanol sample, as outlined in the Bruker VTU user manual.

Herein, numbered proton and carbon atoms refer to the positions of the C_5H_4 rings and the phenylene linker within the FcPPB ligand backbone. The C_5H_4 ring bound to the $C_5H_4P(^t\text{Bu})Ar$ phosphine was numbered $C^{1'\text{-}5'}$, where $C^{1'}$ is the *ipso*-carbon atom bound to phoshorus, and the C_5H_4 ring bound to the $C_5H_4PPh_2$ phosphine was numbered $C^{1''\text{-}5''}$, where $C^{1''}$ is the *ipso*-carbon atom bound to phosphorus. Prior to installation of the $-BPh_2$ group, the phenylene linker was numbered such that C^1 refers to the carbon atom bound to Br, and C^2 refers to the carbon atom bound to phosphine moiety. Following installation of the $-BPh_2$ group, the phenylene linker was numbered such that C^1 refers to the carbon atom bound to the phosphine moiety, and C^2 refers to the carbon atom bound to the borane. The remainder of the carbon atoms and protons in the phenylene linker were numbered accordingly in both cases. Inequivalent phenyl rings on boron and phosphorus are labeled A and B so that the proton and carbon resonances belonging to a single phenyl ring can be identified. We did not identify which *P*- or *B*-phenyl rings give rise to the signals labeled A or B, respectively.

X-ray crystallographic analyses were performed on suitable crystals coated in Paratone oil and mounted on a SMART APEX II diffractometer with a 3 kW Sealed tube Mo generator in the McMaster Analytical X-Ray (MAX) Diffraction Facility. In all cases, non-hydrogen atoms were refined anisotropically and hydrogen atoms were generated in ideal positions and then updated with each cycle of refinement, with the only exception being H(46) in **6A**·$4C_6H_6$, which was located in the difference map. One molecule of C_6H_6 in **6A**·$4C_6H_6$ was positionally disordered over two positions in a 58:42 ratio. The disorder was modeled allowing occupancy and positional parameters to refine freely; carbon atoms were restrained to have similar thermal parameters through the use of the SIMU command. CCDC-1019205-1019209 contains the supplementary crystallographic data for this paper. These data can be obtained free of charge from The Cambridge Crystallographic Data Centre via www.ccdc.cam.ac.uk/data%5Frequest/cif.

$(o\text{-}BrC_6H_4)P(NEt_2)_2$: Tetrahydrofuran (50 mL) and diethylether (50 mL) were condensed into a 250 mL two-necked round bottom flask using a dry ice/acetone bath, to which 1,2-dibromobenzene (6.86 g, 29.1 mmol) in tetrahydrofuran (10 mL) was added via syringe. The solution was cooled to –110 °C through the use of a diethyl ether/liquid nitrogen bath, and a solution of *n*BuLi in hexanes (18 mL, 1.6 M) was added dropwise over 20 minutes. The reaction mixture was maintained at –110 °C for 2 hours, after which point a solution of $Cl\text{–}P(NEt_2)_2$ (6.13 g, 29.1 mmol) in THF (20 mL) was added dropwise over 10 minutes. The reaction mixture was maintained at –110 °C for an additional hour before warming to room temperature overnight. The resulting light orange, opaque solution was evaporated to dryness *in vacuo* to yield an opaque, orange oil. Hexanes (100 mL) were added to the crude oil and the resulting slurry was sonicated and filtered to remove any unwanted LiCl, which was washed with hexanes (2 × 20 mL). The clear and light yellow filtrate was evaporated to dryness *in vacuo* to yield a translucent, fawn yellow oil. Yield = 9.26 g (96%). ^{1}H NMR (500 MHz, [D$_6$]benzene, 25 °C): δ = 7.49 (dt, ^3J(H,H) = 8 Hz, ^3J(H,P) = 2 Hz, 1H; CH^3), 7.44 (ddd, ^3J(H,H) = 8 Hz, ^4J(H,P) = 5 Hz, ^4J(H,H) = 1 Hz, 1H; CH^6), 7.08 (t, ^3J(H,H) = 8 Hz, 1H; CH^4), 6.78 (tt, ^3J(H,H) = 8 Hz, ^4J(H,H) = 2 Hz, 1H; CH^5), 3.09–2.94 (m, 8H; N(CH_2CH$_3$)$_2$), 1.02 (t, ^3J(H,H) = 7 Hz, 12H; N(CH$_2$CH_3)$_2$); ^{13}C{^{1}H} NMR (126 MHz, [D$_6$]benzene, 25 °C): δ = 143.9 (d, ^2J(C,P) = 15 Hz; C^2), 134.5 (s; C^6), 133.3 (d, ^2J(C,P) = 6 Hz; C^3), 129.9 (s; C^5), 128.2 (d, ^1J(C,P) = 30 Hz; C^1), 127.6 (s; C^4), 44.7 (d, ^2J(C,P) = 19 Hz; N(CH_2CH$_3$)$_2$), 15.8 (d, ^3J(C,P) = 3 Hz; N(CH$_2$$CH_3$)$_2$); ^{31}P{^{1}H} NMR (203 MHz, [D$_6$]benzene, 25 °C): δ = 96.4 (s) MS: calcd for $C_{14}H_{24}BrN_2P$: 331.2217 [M$^+$]; found: 332.0854.

$(o\text{-}BrC_6H_4)PCl_2$: Tetrahydrofuran (200 mL) was condensed into a 500 mL two-necked round bottom flask using a dry ice/acetone bath, to which a solution of $(o\text{-}BrC_6H_4)P(NEt_2)_2$ (9.01 g, 27.2 mmol) in tetrahydrofuran (20 mL) was added via syringe. A solution of HCl in dioxanes (54 mL, 4.0 M) was then added dropwise at room temperature, which resulted in the immediate formation of a white precipitate; the reaction mixture was left to stir for 1 hour at room temperature. Next, the reaction mixture was evaporated to dryness *in vacuo* to yield an opaque, white oil. Diethyl ether (80 mL) was added to the crude oil and the resulting slurry was sonicated and filtered to remove any unwanted $HCl{\cdot}HNEt_2$, which was washed with diethyl ether (1 × 20 mL). The clear and colourless filtrate was evaporated to dryness *in vacuo* to yield a translucent, fawn yellow oil. Yield = 6.35 g (91%). ^{1}H NMR (500 MHz, [D$_6$]benzene, 25 °C): δ = 7.80

(appt. d, ^3J(H,H) = 8 Hz, 1H; CH^3), 7.00 (ddd, ^3J(H,H) = 8 Hz, ^4J(H,P) = 5 Hz, ^4J(H,H) = 1 Hz, 1H; CH^6), 6.81 (t, ^3J(H,H) = 8 Hz, 1H; CH^4), 6.60 (dt, ^3J(H,H) = 8 Hz, ^4J(H,H) = 2 Hz, 1H; CH^5); ^{13}C{^{1}H} NMR (126 MHz, [D$_6$]benzene, 25 °C): δ = 140.2 (d, ^1J(C,P) = 57 Hz; C^2), 134.2 (s; C^5), 133.5 (s; C^6), 132.4 (d, ^2J(C,P) = 5 Hz; C^3), 128.9 (s; C^4), 127.2 (d, ^2J(C,P) = 45 Hz; C^1); ^{31}P{^{1}H} NMR (203 MHz, [D$_6$]benzene, 25 °C): δ = 153.7 (s); MS: calcd for $C_6H_4BrCl_2P$: 257.8749 [M$^+$]; found: 257.8601.

(*o*-BrC$_6$H$_4$)^{t}BuPCl: Diethyl ether (100 mL) was condensed into a 250 mL two-necked round bottom flask equipped with a reflux condenser using a dry ice/acetone bath, to which (*o*-BrC$_6$H$_4$)PCl$_2$ (6.31 g, 24.5 mmol) in diethyl ether (20 mL) was added via syringe. The solution was cooled to –20 °C through the use of a brine/liquid nitrogen bath, and a solution of ^{t}BuMgBr in diethyl ether (12 mL, 2.0 M) was added dropwise over 10 minutes (the addition of ^{t}BuMgBr resulted in the formation of a white precipitate). The reaction mixture was maintained at –20 °C for 30 minutes and then refluxed for 6 hours. The resulting light orange, opaque solution was evaporated to dryness *in vacuo* to yield a white/yellow oil. At this point, the reflux condenser was replaced with a swivel frit and diethyl ether (80 mL) was added to the crude oil; the resulting slurry was sonicated and filtered to remove any unwanted MgBrCl, which was washed with diethyl ether (2 × 10 mL). The clear, light yellow filtrate was evaporated to dryness *in vacuo* to yield a translucent, fawn yellow oil, which was then distilled *in vacuo* at 130 °C to yield a clear, colourless oil. Yield = 4.71 g (69%). ^{1}H NMR (500 MHz, [D$_6$]benzene, 25 °C): δ = 7.72 (dt, ^3J(H,H) = 8 Hz, ^4J(H,P) = 2 Hz, 1H; CH^6), 7.22 (ddd, ^3J(H,H) = 8 Hz, ^3J(H,P) = 4 Hz, ^4J(H,H) = 1 Hz, 1H; CH^3), 6.90 (dt, ^3J(H,H) = 8 Hz, ^4J(H,H) = 1 Hz, 1H; CH^5), 6.66 (t, ^3J(H,H) = 7 Hz, 1H; CH^4), 1.02 (d, ^3J(H,P) = 13 Hz, 9H; CMe_3); ^{13}C{^{1}H} NMR (126 MHz, [D$_6$]benzene, 25 °C): δ = 137.3 (d, ^1J(C,P) = 46 Hz; C^2), 134.5 (s; C^6), 133.0 (d, ^2J(C,P) = 1 Hz; C^3), 131.7 (s; C^4), 129.6 (d, ^2J(C,P) = 42 Hz; C^1), 127.2 (s; C^5), 36.4 (d, ^1J(C,P) = 33 Hz; CMe_3), 25.8 (d, ^2J(C,P) = 17 Hz, CMe_3); ^{31}P{^{1}H} NMR (203 MHz, [D$_6$]benzene, 25 °C): δ = 105.5 (s); MS: calcd for $C_{10}H_{13}BrClP$: 279.5337 [M$^+$]; found: 279.9598.

[Fe(η^5-C$_5$H$_4$PPh$_2$){η^5-C$_5$H$_4$P(^{t}Bu)(*o*-BrC$_6$H$_4$)}] · 0.4pentane: Tetrahydrofuran (125 mL) was condensed into a 250 ml two-necked round bottom flask containing [Fe(η^5-C$_5$H$_4$Br)(η^5-C$_5$H$_4$PPh$_2$)] (3.62 g, 8.07 mmol) through the use of a dry ice/acetone bath. The tetrahydrofuran solution was cooled to –78°C and a solution of *n*BuLi in hexanes (5.0 mL, 1.6 M) was added dropwise, causing the transparent, orange solution to turn crimson red. The reaction mixture was left to stir at –78°C for 2 hours, after which a solution of (*o*-BrC$_6$H$_4$)P(^{t}Bu)Cl (2.26 g, 8.07 mmol) in tetrahydrofuran (10 mL) was added dropwise. The reaction mixture was then left to stir overnight at room temperature. After stirring overnight the transparent, crimson red solution was evaporated to dryness *in vacuo* to yield a bright red oil. Hexanes (100 mL) was added to the oil and the resulting slurry was sonicated, which resulted in the precipitation of LiCl. The hexanes solution was filtered to remove LiCl and the filtrate was evaporated to dryness *in vacuo* to again yield an orange/red oil. The crude oil was brought into the dry box and recrystallized from pentane, which yielded [Fe(η^5-C$_5$H$_4$PPh$_2$){η^5-C$_5$H$_4$P(^{t}Bu)(*o*-BrC$_6$H$_4$)}] · 0.4pentane as an orange/yellow solid. Yield = 3.83 g (74%). ^{1}H NMR (600 MHz, [D$_6$]benzene, 25 °C): δ = 7.47 (dd, ^3J(P,H) = 4 Hz, ^3J(H,H) = 1 Hz, 1H; CH^3), 7.46–7.43 (m, 4H; *o*-PPh_2), 7.42 (d, ^3J(H,H) = 2 Hz, 1H; CH^6), 7.07–7.03 (m, 6H; *m*+*p*-PPh_2), 6.87 (dt, ^3J(H,H) = 8 Hz, ^4J(H,H) = 1 Hz, 1H; CH^5), 6.71 (ddt, ^3J(H,H) = 8 Hz, ^4J(H,P) = 2 Hz, ^4J(H,H) = 1 Hz, 1H; CH^4), 4.35 (septet, ^3J(H,H) = 1 Hz, 1H; C$H^{5'/2'}$), 4.23 (sextet, ^3J(H,H) = 1 Hz, 1H; C$H^{3''/4''}$), 4.20 (septet, ^3J(H,H) = 1 Hz, 1H; C$H^{4'/3'}$), 4.15 (sextet, ^3J(H,H) = 1 Hz, 1 H; C$H^{3'/4'}$), 4.15–4.13 (m, 2H; C$H^{2''/5''}$, C$H^{4''/3''}$), 4.04 (sextet, ^3J(H,H) = 1 Hz, 1H; C$H^{2'/5'}$), 3.87 (octet, ^3J(H,H) = 1 Hz, 1H; C$H^{5''/2''}$), 1.10 (d, ^3J(H,P) = 12 Hz, 9H; CMe_3); ^{13}C{^{1}H} NMR (151 MHz, [D$_6$]benzene, 25 °C): δ = 140.0 (appt. t, ^1J(C,P) = 12 Hz; *ipso*-PPh_2), 139.7 (d, ^2J(C,P) = 22 Hz; C^1), 137.1 (s; C^6), 134.0 (appt. t, ^2J(C,P) = 20 Hz; *o*-PPh_2), 133.4 (d, ^2J(C,P) = 3 Hz; C^3), 133.2 (d, ^1J(C,P) = 40 Hz; C^2), 130.5 (s; C^4), 128.7 (d, ^3J(C,P) = 4 Hz; *p*-PPh_2), 128.5 (appt. t, ^3J(C,P) = 6 Hz; *m*-PPh_2), 126.4 (s; C^5), 77.4 (d, ^1J(C,P) = 9 Hz; $C^{1''}$), 76.3 (d, ^1J(C,P) = 22 Hz; $C^{1'}$), 76.2 (d, ^3J(C,P) = 28 Hz; $C^{5''/2'}$), 74.5 (d, ^2J(C,P) = 16 Hz; $C^{2''/5''}$), 74.1 (d, ^2J(C,P) = 14 Hz; $C^{5''/2''}$), 73.5 (s; $C^{3''/4''}$), 73.3 (s; $C^{4''/3''}$), 73.2 (d, ^2J(C,P) = 4 Hz; $C^{2'/5'}$), 72.8 (s; $C^{3'/4'}$), 72.0 (d, ^2J(C,P) = 6 Hz; $C^{4'/3'}$), 32.6 (d, ^1J(C,P) = 16 Hz; CMe_3), 28.5 (d, ^2J(C,P) = 16 Hz; CMe_3); ^{31}P{^{1}H} NMR (203 MHz, [D$_6$]benzene, 25 °C): δ = 4.9 (s; C$_5$H$_4$*P*(^{t}Bu)Ar), –17.0 (s; C$_5$H$_4$*P*Ph$_2$); elemental analysis calcd (%) for $C_{34}H_{35.8}BrFeP_2$: C 63.59, H 5.62; found: C 63.50, H 5.75.

FcPPB: Toluene (120 mL) was condensed into a 250 ml round bottom flask containing [Fe(η^5-C$_5$H$_4$PPh$_2$){η^5-C$_5$H$_4$P(^{t}Bu)(*o*-BrC$_6$H$_4$)}]·0.4pentane (1.54 g, 2.40 mmol) through the use of a dry ice/acetone bath. The toluene solution was cooled to –45°C and a solution of ^{t}BuLi (0.32 g, 5.0 mmol) in toluene (5 mL) was added dropwise. The reaction mixture was then warmed to 0°C and left to stir at that temperature for 3.5 hours, during which time a fine, white solid precipitated from solution, turning the previously transparent, orange solution translucent. The reaction mixture was then cooled to –45°C and a solution of Br–BPh$_2$ (0.61 g, 2.5 mmol) in toluene (5 mL) was added dropwise; the reaction mixture was then left to stir overnight at room temperature. After stirring overnight the opaque, tangerine coloured solution was evaporated to dryness *in vacuo* to yield a red/orange oil. The crude oil was brought into the dry box, at which point toluene (30 mL) was added to precipitate out LiBr. The crude mixture was centrifuged to separate LiBr from the desired FcPPB ligand, and the clear orange mother liquors were evaporated to dryness *in vacuo* to again yield a red/orange oil. Hexanes (50 mL) were added to the oil and the resulting slurry was sonicated, which resulted in the precipitation of FcPPB as a light yellow solid. The hexanes solution was filtered, and the collected FcPPB ligand was washed with hexanes (2 × 10 mL). Yield = 1.36 g (78 %). ^{1}H NMR (600 MHz, [D$_6$]benzene, 25 °C): δ = 7.95 (broad d, ^3J(H,H) = 5 Hz, 2H; *o*-BPh_2 A), 7.86 (broad d, ^3J(H,H) = 5 Hz, 2H; *o*-BPh_2 B), 7.82 (d, ^3J(H,H) = 7 Hz, 1H; CH^3), 7.42 (ddt, ^3J(H,H) = 7 Hz, ^4J(H,H) = 3 Hz, ^5J(H,P) = 1 Hz, 1H; CH^4), 7.39–7.36 (m, 2H; *o*-PPh_2 A), 7.31–7.28 (m, 4H; *o*-BPh_2 B, *m*-BPh_2 A), 7.23 (appt. tt, ^3J(H,H) = 8 Hz, ^2J(H,P) = 1 Hz, 3H; *m*-BPh_2 B, CH^6), 7.19 (ddt, ^3J(H,H) = 7 Hz, ^4J(H,P) = 3 Hz, ^4J(H,H) = 1 Hz, 1H; CH^5), 7.15–7.12 (m, 2H; *p*-BPh_2 A+B), 7.06 (dt, ^3J(H,H) = 3 Hz, ^4J(H,H) = 1 Hz, 3H; *m*+*p*-PPh_2 A), 7.02–7.01 (m, 3H; *m*+*p*-PPh_2 B), 4.34 (sextet, ^3J(H,H) = 1 Hz, 1H; C$H^{2'/5'}$), 4.25 (sextet, ^3J(H,H) = 1 Hz, 1H; C$H^{4'/3'}$), 4.12 (septet, ^3J(H,H) = 1 Hz, 1H; C$H^{3'/4'}$), 4.08 (sextet, ^3J(H,H) = 1 Hz, 1H; C$H^{5'/2'}$), 3.59 (septet, ^3J(H,H) = 1 Hz, 1H; C$H^{2''/5''}$), 3.43 (sextet, ^3J(H,H) = 1 Hz, 1H; C$H^{5''/2''}$), 3.29 (sextet, ^3J(H,H) = 1 Hz, 1H; C$H^{3''/4''}$), 3.22 (sextet, ^3J(H,H) = 1Hz, 1H; C$H^{4''/3''}$), 0.76 (d, ^3J(H,P) = 14 Hz, 9H; CMe_3); ^{13}C{^{1}H} NMR (151 MHz, [D$_6$]benzene, 25 °C): δ = 164.9

(broad d, ^2J(C,P) = 43 Hz; *C*^{2}), 149.5 (broad s; *ipso*-B*Ph*$_2$ A or B), 148.2 (broad s; *ipso*-B*Ph*$_2$ A or B), 140.0 (d, ^1J(C,P) = 12 Hz; *ipso*-P*Ph*$_2$ B), 139.2 (d, ^1J(C,P) = 12 Hz; *ipso*-P*Ph*$_2$ A), 135.7 (d, ^1J(C,P) = 45 Hz; *C*^{1}), 134.8 (broad s; *o*-B*Ph*$_2$ B), 134.2 (d, ^2J(C,P) = 20 Hz; *o*-P*Ph*$_2$ A), 133.7 (d, ^2J(C,P) = 20 Hz; *o*-P*Ph*$_2$ B), 133.4 (broad s; *o*-B*Ph*$_2$ A), 132.0 (s; *C*^{4}), 131.9 (s; *C*^{3}), 129.3 (s; *m*-B*Ph*$_2$ B), 128.4 (s; *p*-P*Ph*$_2$ A), 128.4 (d, ^3J(C,P) = 7 Hz; *m*-P*Ph*$_2$ A), 128.3 (d, ^3J(C,P) = 7 Hz; *m*-P*Ph*$_2$ B), 128.2 (s; *p*-P*Ph*$_2$ B), 127.6 (s; *m*-B*Ph*$_2$ A, *C*^{6}), 127.5 (d, ^3J(C,P) = 6 Hz; *C*^{5}), 126.9 (broad s; *p*-B*Ph*$_2$ A or B), 126.1 (broad s; *p*-B*Ph*$_2$ A or B), 77.7 (d, ^1J(C,P) = 8 Hz; *C*$^{1''}$), 75.9 (d, ^2J(C,P) = 20 Hz; *C*$^{2'/5'}$), 74.5 (s; *C*$^{3''/4''}$), 74.4 (d, ^2J(C,P) = 14 Hz; *C*$^{2''/5''}$), 73.8 (s; *C*$^{4''/3''}$), 73.6 (d, ^2J(C,P) = 3 Hz; *C*$^{5''/2''}$), 73.5 (d, ^2J(C,P) = 10 Hz; *C*$^{5'/2'}$), 72.8 (s; *C*$^{4'/3'}$), 72.4 (d, ^3J(C,P) = 9 Hz; *C*$^{3'/4'}$), 70.6 (d, ^1J(C,P) = 16 Hz; *C*$^{1'}$), 34.2 (d, ^1J(C,P) = 7 Hz; *C*Me$_3$), 27.4 (d, ^2J(C,P) = 4 Hz; C*Me*$_3$); ^{31}P{^{1}H} NMR (203 MHz, [D$_6$]benzene, 25 °C): *δ* = 19.7 (s; C$_5$H$_4$*P*(^{t}Bu)Ar), –17.2 (s; C$_5$H$_4$*P*Ph$_2$); ^{11}B NMR (161 MHz, [D$_6$]benzene, 25 °C)**:** *δ* = 17 (broad s, ω$_{1/2}$ = 1300 Hz); elemental analysis calcd (%) for $C_{44}H_{41}BFeP_2$: C 75.67, H 5.92; found: C 75.70, H 6.12.

[Pt(FcPPB)]·0.3hexanes (1): Toluene (50 mL) was condensed into a round bottom flask containing [Pt(nb)$_3$] (351 mg, 0.734 mmol) and FcPPB (513 mg, 0.734 mmol) through the use of a dry ice/acetone bath. The fawn yellow reaction solution was left to stir for 5 hours at room temperature before being evaporated to dryness *in vacuo*. Hexanes (50 mL) were condensed into the reaction flask and the oily suspension was sonicated for 15 minutes, after which point the hexanes solution was filtered and the product was collected as a fawn yellow solid. The collected product was washed with hexanes (2×10 mL) Yield = 515 mg (76%). ^{1}H NMR (600 MHz, [D$_2$]methylene chloride, 25 °C): *δ* = 8.01 (d, ^3J(H,H) = 7 Hz, 1H; C*H*^{6}), 7.94 (broad s, 2H; *o*-P*Ph*$_2$ A), 7.62 (d, ^3J(H,H) = 7 Hz, 2H; *o*-B*Ph*$_2$ A), 7.53 (s, 3H; *m*+*p*-P*Ph*$_2$ A), 7.49 (t, ^3J(H,H) = 7 Hz, 1H; C*H*^{5}), 7.28–7.22 (m, 3H; *m*+*p*-P*Ph*$_2$ B), 7.16–7.12 (m, 3H; C*H*^{4}, *m*-B*Ph*$_2$ A), 7.00 (t, ^3J(H,H) = 7 Hz, 1H; *p*-B*Ph*$_2$ A), 6.90 (t, ^3J(H,H) = 8 Hz, 1H; C*H*^{3}), 6.79 (t, ^3J(H,H) = 9 Hz, 2H; *o*-P*Ph*$_2$ B), 6.65 (t, ^3J(H,H) = 7 Hz, 2H; *m*-B*Ph*$_2$ B), 6.19 (t, ^3J(H,H) = 7 Hz, 1H; *p*-B*Ph*$_2$ B), 6.10 (t, ^3J(H,H) = 5 Hz, 2H; *o*-B*Ph*$_2$ B), 4.60 (s, 1H; C*H*$^{5'/2'}$), 4.36 (s, 1H; C*H*$^{5''/2''}$), 4.33 (s, 1H; C*H*$^{4''/3''}$), 4.27 (s, 1H; C*H*$^{3'/4'}$), 4.23 (s, 1H; C*H*$^{4'/3'}$), 4.16 (s, 1H; C*H*$^{3''/4''}$), 3.93 (s, 1H; C*H*$^{2'/5'}$), 3.79 (s, 1H; C*H*$^{2''/5''}$), 1.07 (d, ^3J(H,P) = 12 Hz, 9H; C*Me*$_3$); ^{13}C{^{1}H} NMR (151 MHz, [D$_2$]methylene chloride, 25 °C): δ = 161.9 (broad d, ^2J(C,P) = 38 Hz; *C*^{2}), 149.6 (appt. broad d, *J* = 15 Hz; *ipso*-B*Ph*$_2$ A), 148.0 (dd, ^1J(C,P) = 50 Hz, ^3J(C,P) = 13 Hz; *C*^{1}), 137.3 (d, ^1J(C,P) = 41 Hz; *ipso*-PPh$_2$ A), 136.1 (d, ^2J(C,P) = 16 Hz; *o*-P*Ph*$_2$ A), 134.9 (dd, ^1J(C,P) = 35 Hz, ^3J(C,P) = 4 Hz; *ipso*-P*Ph*$_2$ B), 134.3 (s; *C*^{3}), 133.9 (dd, ^2J(C,P) = 28 Hz, ^4J(C,P) = 3 Hz; *C*^{6}), 132.3 (d, ^2J(C,P) = 13 Hz; *o*-P*Ph*$_2$ B), 132.2 (s; *o*-B*Ph*$_2$ A), 131.1 (s; *p*-P*Ph*$_2$ A), 129.9 (s; *C*^{5}), 129.7 (s; *m*-B*Ph*$_2$ B), 129.0 (s; *p*-P*Ph*$_2$ B), 129.0 (appt. s; *m*-P*Ph*$_2$ A), 128.0 (d, ^3J(C,P) = 10 Hz; *m*-P*Ph*$_2$ B), 126.9 (s; *m*-B*Ph*$_2$ A), 125.9 (appt. d, *J* = 5 Hz; *p*-B*Ph*$_2$ B), 125.3 (d, ^4J(C,P) = 7 Hz; *C*^{4}), 124.7 (s; *p*-B*Ph*$_2$ A), 114.2 (broad s; *ipso*-B*Ph*$_2$ B), 113.5 (broad s; *o*-B*Ph*$_2$ B), 83.7 (d, ^1J(C,P) = 45 Hz; *C*$^{1'}$), 82.7 (d, ^1J(C,P) = 51 Hz; *C*$^{1''}$), 76.3 (d, ^2J(C,P) = 13 Hz; *C*$^{2'/5'}$), 74.7 (d, ^2J(C,P) = 13 Hz; *C*$^{2''/5''}$), 74.5 (d, ^3J(C,P) = 8 Hz; *C*$^{5''/2''}$), 72.9 (d, ^3J(C,P) = 3 Hz; *C*$^{5'/2'}$), 71.5 (d, ^2J(C,P) = 7 Hz; *C*$^{3'/4'}$), 71.2 (d, ^3J(C,P) = 4 Hz; *C*$^{4''/3''}$), 70.1 (d, ^2J(C,P) = 6 Hz; *C*$^{3''/4''}$), 69.9 (d, ^3J(C,P) = 3 Hz; *C*$^{4'/3'}$), 37.1 (d, ^1J(C,P) = 26 Hz; *C*Me$_3$), 29.7 (d, ^2J(C,P) = 6 Hz; C*Me*$_3$); ^{31}P{^{1}H} NMR (243 MHz, [D$_6$]benzene, 25 °C): *δ* = 50.8 (d, ^1J(P,Pt) = 5651 Hz, ^2J(P,P) = 56 Hz; C$_5$H$_4$*P*(^{t}Bu)Ar), 28.5 (d, ^1J(P,Pt) = 4183 Hz, ^2J(P,P) = 56 Hz; C$_5$H$_4$*P*Ph$_2$); ^{31}P{^{1}H} NMR (203 MHz, [D$_2$]methylene chloride, 25 °C): *δ* = 51.3 (d, ^1J(P,Pt) = 5657 Hz, ^2J(P,P) = 55 Hz; C$_5$H$_4$*P*(^{t}Bu)Ar), 28.4 (d, ^1J(P,Pt) = 4157 Hz, ^2J(P,P) = 55 Hz; C$_5$H$_4$*P*Ph$_2$); ^{11}B NMR (161 MHz, [D$_2$]methylene chloride, 25 °C)**:** *δ* = 21 (broad s, ω$_{1/2}$ = 1400 Hz); ^{195}Pt{^{1}H} NMR (128 MHz, [D$_2$]methylene chloride, 25 °C): *δ* –4934 (dd, ^1J(Pt,P) = 5654 Hz, ^1J(Pt,P) = 4138 Hz); elemental analysis calcd (%) for $C_{45.8}H_{44.2}BFeP_2Pt$: C 59.84, H 4.96; found: C 59.93, H 5.27.

[Pt(CO)(FcPPB)] (2): A solution of [Pt(FcPPB)] · 0.3hexanes (64.7 mg, 7.04×10^{-2} mmol) in CH_2Cl_2 (5 mL) was subject to three freeze/pump/thaw cycles before being cooled to –140 °C, at which point CO was added. The reaction mixture was stirred for one hour at room temperature before being evaporated to dryness *in vacuo* to yield a brown/yellow oily residue. Hexanes (20 mL) were added to the crude product and the resulting solution was sonicated for 15 minutes, after which point the resulting solution was evaporated to dryness *in vacuo* to yield a mustard yellow solid. Yield = 38 mg (58 %). ^{1}H NMR (600 MHz, [D$_6$]benzene, 25 °C): *δ* = 8.12 (d, ^3J(H,H) = 7 Hz, 2H; *o*-B*Ph*$_2$ A), 7.83–7.80 (m, 2H; *o*-P*Ph*$_2$ A), 7.66 (d, ^3J(H,P) = 8 Hz, 1H; C*H*^{6}), 7.47 (t, ^3J(H,H = 8 Hz, 2H; *m*-B*Ph*$_2$ A), 7.35 (t, ^3J(H,H) = 7 Hz, 1H; C*H*^{3}), 7.30–7.28 (m, 3H; *o*-B*Ph*$_2$ B, *p*-B*Ph*$_2$ A), 7.18–7.12 (m, 3H; C*H*^{5}, *o*-P*Ph*$_2$ B), 7.08–7.05 (m, 1H; C*H*^{4}), 7.04–7.00 (m, 3H; *m*+*p*-P*Ph*$_2$ A), 6.89–6.83 (m, 4H; *p*-B*Ph*$_2$ B, *m*+*p*-P*Ph*$_2$ B), 6.64 (t, ^3J(H,H) = 8 Hz, 2H; *m*-B*Ph*$_2$ B), 4.51 (s, 1H; C*H*$^{5'/2'}$), 4.49 (d, ^3J(H,H) = 1 Hz, 1H; C*H*$^{2'/5'}$), 4.03–4.01 (m, 1H; C*H*$^{2''/5''}$), 4.01–4.00 (m, 1H; C*H*$^{5''/2''}$), 3.91 (sextet, ^3J(H,H) = 1 Hz, 1H; C*H*$^{3''/4''}$), 3.85 (sextet, ^3J(H,H) = 1 Hz, 1H; C*H*$^{4'/3'}$), 3.81 (q, ^3J(H,H) = 2 Hz, 1H; C*H*$^{3'/4'}$), 3.73 (sextet, ^3J(H,H) = 1 Hz, 1H; C*H*$^{4''/3''}$), 1.31 (d, ^3J(H,P) = 15 Hz, 9H; C*Me*$_3$); ^{13}C{^{1}H} NMR (151 MHz, [D$_6$]benzene, 25 °C): *δ* = 193.6 (dd, ^2J(C,P) = 87 Hz, ^2J(C,P) = 9 Hz; Pt-*C*O), 165.5 (broad d, ^2J(C,P) = 45 Hz; *C*^{2}), 153.0 (broad s; *ipso*-B*Ph*$_2$ A), 140.1 (s; *o*-B*Ph*$_2$ B), 138.9 (dd, ^1J(C,P) = 49 Hz, ^3J(C,P) = 11 Hz; *C*^{1}), 138.4 (d, ^1J(C,P) = 32 Hz; *ipso*-P*Ph*$_2$ B), 136.9 (s; *o*-B*Ph*$_2$ A), 136.2 (d, ^1J(C,P) = 36 Hz; *ipso*-P*Ph*$_2$ A), 135.2 (d, ^2J(C,P) = 15 Hz; *o*-P*Ph*$_2$ A), 134.5 (d, ^2J(C,P) = 26 Hz; *C*^{6}), 132.9 (d, ^2J(C,P) = 14 Hz; *o*-P*Ph*$_2$ B), 130.9 (s; *C*^{3}), 130.5 (d, ^2J(C,P) = 9 Hz; *m*-P*Ph*$_2$ A), 130.3 (broad s; *ipso*-B*Ph*$_2$ B), 129.0 (s; *p*-P*Ph*$_2$ B), 128.2 (s, *C*^{5}; *p*-P*Ph*$_2$ A), 128.1 (s; *p*-B*Ph*$_2$ B), 127.7 (d, ^3J(C,P) = 10 Hz; *m*-P*Ph*$_2$ B), 127.3 (s; *m*-B*Ph*$_2$ A), 126.0 (s; *m*-B*Ph*$_2$ B), 125.7 (s; *p*-B*Ph*$_2$ A), 125.3 (d, ^4J(C,P) = 7 Hz; *C*^{4}), 86.9 (dd, ^1J(C,P) = 36 Hz, ^3J(C,P) = 6 Hz; *C*$^{1'}$), 86.0 (d, ^1J(C,P) = 41 Hz; *C*$^{1''}$), 75.4 (d, ^2J(C,P) = 7 Hz; *C*$^{5'/2'}$), 75.0 (s; *C*$^{3''/4''}$), 74.8 (d, ^2J(C,P) = 20 Hz; *C*$^{2''/5''}$), 72.1 (d, ^2J(C,P) = 8 Hz; *C*$^{5''/2''}$), 71.5 (d, ^2J(C,P) = 7 Hz; *C*$^{2'/5'}$), 70.1 (d, ^3J(C,P) = 4 Hz; *C*$^{3'/4'}$), 69.2 (s; *C*$^{4''/3''}$), 69.0 (d, ^3J(C,P) = 4 Hz; *C*$^{4'/3'}$), 37.9 (d, ^1J(C,P) = 31 Hz; *C*Me$_3$), 29.4 (d, ^2J(C,P) = 6 Hz; C*Me*$_3$); ^{31}P{^{1}H} NMR (203 MHz, [D$_6$]benzene, 25 °C): *δ* = 59.4 (s, ^1J(P,Pt) = 4884 Hz; C$_5$H$_4$*P*(^{t}Bu)Ar), 22.8 (s, ^1J(Pt,P) = 2343 Hz; C$_5$H$_4$*P*Ph$_2$); ^{11}B NMR (161 MHz, [D$_6$]benzene, 25 °C): *δ*= 21 (broad s, ω$_{1/2}$ = 1550 Hz); ^{11}B NMR (161 MHz, [D$_2$]methylene chloride, 25 °C): *δ* = 19 (broad s, ω$_{1/2}$ = 1550 Hz); ^{195}Pt{^{1}H} NMR (128 MHz, [D$_2$]methylene chloride, 25 °C): *δ* –4422 (dd, ^1J(Pt,P) = 4820 Hz, ^1J(Pt,P) = 2223 Hz); IR (CH_2Cl_2): ν = 1982 cm^{-1} (C≡O); IR (nujol): ν = 1994, 1968 cm^{-1} (C≡O); elemental analysis calcd (%) for $C_{45}H_{41}BFeOP_2Pt$: C 58.65, H 4.49; found: C 57.94, H 4.68.

[Pt(CNXyl)(FcPPB)] (3): A solution of XylNC (15.4 mg, 0.118 mmol) in CH_2Cl_2 (3 mL) was added dropwise at room

temperature to a solution of [Pt(FcPPB)]·0.3hexanes (105 mg, 0.114 mmol) in CH_2Cl_2 (10 mL). The transparent, orange/red solution was left to stir for one hour at room temperature before being evaporated to dryness *in vacuo*. Hexanes (20 mL) were added to the remaining orange/red oily residue and the resulting solution was sonicated for 15 minutes, which resulted in the precipitation of [Pt(CNXyl)(FcPPB)] as a yellow powder. The hexanes solution was filtered and the collected product was washed with hexanes (2×10 mL). Yield = 101 mg (87%). ^{1}H NMR (600 MHz, [D$_6$]benzene, 25 °C): δ = 8.26 (d, ^3J(H,H) = 7 Hz, 2H; *o*-B*Ph*$_2$ A), 8.01 (dt, ^3J(H,P) = 10 Hz, ^3J(H,H) = 1 Hz, 2H; *o*-P*Ph*$_2$ A), 7.73 (d, ^3J(H,P) = 8 Hz, 1H; C*H*^{6}), 7.54 (d, ^3J(H,H) = 7 Hz, 2H; *o*-B*Ph*$_2$ B), 7.30 (t, ^3J(H,H) = 8 Hz, 2H; *m*-B*Ph*$_2$ A), 7.22–7.13 (m, 6H; C*H*^{3}, C*H*^{5}, *o*-P*Ph*$_2$ B, *m*-B*Ph*$_2$ B), 7.08–7.03 (m, 5H; C*H*^{4}, *m*-P*Ph*$_2$ A, *p*-B*Ph*$_2$ A and B), 7.00–6.96 (m, 3H; *m*-P*Ph*$_2$ B, *p*-P*Ph*$_2$ A), 6.91 (tq, ^3J(H,H) = 7 Hz, ^4J(H,H) = 1 Hz, 1H; *p*-P*Ph*$_2$ B), 6.65 (t, ^3J(H,H) = 8 Hz, 1H; *p*-Xyl), 6.55 (d, ^3J(H,H) = 8 Hz, 2H; *m*-Xyl), 4.79 (septet, ^3J(H,H) = 1 Hz, 1H; C*H*$^{2'/5'}$), 4.52 (s, 1H; C*H*$^{5'/2'}$), 4.22 (sextet, ^3J(H,H) = 1 Hz, 1H; C*H*$^{5''/2''}$), 3.95 (t, ^3J(H,H) 2 Hz, 1H; C*H*$^{3'/4'}$), 3.89 (sextet, ^3J(H,H) = 1 Hz, 1H; C*H*$^{4''/3''}$), 3.87 (sextet, ^3J(H,H) = 1 Hz, 1H; C*H*$^{4'/3'}$), 3.81 (sextet, ^3J(H,H) = 1 Hz, 1H; C*H*$^{3''/4''}$), 3.77 (septet, ^3J(H,H) = 1 Hz, 1H; C*H*$^{2''/5''}$), 1.89 (s, 6H; Xyl-C*H*$_3$), 1.47 (d, ^3J(H,P) = 15 Hz, 9H; C*Me*$_3$); ^{13}C{^{1}H} NMR (151 MHz, [D$_6$]benzene, 25 °C): δ = 170.3 (broad d, ^2J(C,P) = 58 Hz; *C*^{2}), 163.9 (d, ^1J(C,P) = 112 Hz; *C*^{1}), 158.7 (broad s; *ipso*-B*Ph*$_2$ A), 149.5 (broad s; *ipso*-B*Ph*$_2$ B), 138.6 (d, ^1J(C,P) = 30 Hz; *ipso*-P*Ph*$_2$ B), 138.0 (s; *o*-B*Ph*$_2$ B), 137.0 (s; *o*-B*Ph*$_2$ A), 136.6 (d, ^1J(C,P) = 27 Hz; *ipso*-P*Ph*$_2$ A), 135.6 (d, ^2J(C,P) = 15 Hz; *o*-PPh$_2$ A), 134.7 (dd, ^2J(C,P) = 27 Hz, ^4J(C,P) = 5 Hz; *C*^{6}), 134.1 (s; *o*-Xyl), 133.4 (d, ^2J(C,P) = 15 Hz; *o*-P*Ph*$_2$ B), 131.1 (s; *C*^{5}), 130.4 (s; *C*^{3}), 130.4 (s; *p*-P*Ph*$_2$ A), 129.1 (s; *p*-P*Ph*$_2$ B), 128.8 (s; *ipso*-Xyl), 128.2 (s; *C*^{4}), 128.1 (d, ^3J(C,P) = 9 Hz; *m*-PPh$_2$ A), 127.9 (d, ^3J(C,P) = 10 Hz; *m*-P*Ph*$_2$ B), 127.6 (s; *m*-Xyl), 127.4 (s; *p*-Xyl), 126.8 (s; *m*-B*Ph*$_2$ A), 126.6 (s; *m*-B*Ph*$_2$ B), 124.6 (s; *p*-B*Ph*$_2$ B), 124.0 (s; *p*-B*Ph*$_2$ A), 86.1 (d, ^1J(C,P) = 36 Hz; *C*$^{1''}$), 85.7 (d, ^1J(C,P) = 8 Hz; C1'), 75.4 (d, ^2J(C,P) = 13 Hz; *C*$^{2''/5''}$), 75.0 (d, ^2J(C,P) = 13 Hz; *C*$^{2'/5'}$), 74.4 (d, ^3J(C,P) = 5 Hz; *C*$^{5''/2''}$), 73.4 (s; *C*$^{5'/2'}$), 71.0 (d, ^2J(C,P) = 7 Hz; *C*$^{3'/4'}$), 70.2 (d, ^2J(C,P) = 5 Hz; *C*$^{3''/4''}$), 69.8 (d, ^3J(C,P) = 2 Hz; *C*$^{4''/3''}$), 69.7 (d, ^3J(C,P) = 2 Hz; *C*$^{4'/3'}$), 36.8 (d, ^1J(C,P) = 34 Hz; *C*Me$_3$), 30.4 (d, ^2J(C,P) = 5 Hz; C*Me*$_3$), 18.5 (s; Xyl-*C*H$_3$); ^{31}P{^{1}H} NMR (203 MHz, [D$_6$]benzene, 25 °C): δ = 62.7 (d, ^1J(P,Pt) = 4549 Hz, ^2J(P,P) 11 Hz; C$_5$H$_4$*P*(^{t}Bu)Ar), 21.8 (d, ^1J(Pt,P) = 1381 Hz, ^2J(P,P) 11 Hz; C$_5$H$_4$*P*Ph$_2$); ^{11}B NMR (161 MHz, [D$_6$]benzene, 25 °C): δ = 13 (broad s, $\omega_{1/2}$ = 800 Hz); ^{11}B NMR (161 MHz, [D$_2$]methylene chloride, 25 °C): δ = 10 (broad s, $\omega_{1/2}$ = 800 Hz); ^{195}Pt{^{1}H} NMR (128 MHz, [D$_6$]benzene, 25 °C): δ –4486 (broad dd, ^1J(Pt,P) = 4632 Hz, ^1J(Pt,P) = 1430 Hz, $\omega_{1/2}$ = 300 Hz); IR (CH_2Cl_2)**:** ν = 2128 cm^{-1} (C≡N); IR (nujol): ν = 2122 cm^{-1} (C≡N); elemental analysis calcd (%) for $C_{53}H_{50}BFeNP_2Pt$: C 62.12; H 4.92; N 1.37; found: C 62.52, H 5.07, N 1.20.

[PtH(μ-H)(FcPPB)] (4): A solution of [Pt(FcPPB)] · 0.3hexanes (25.0 mg, 2.72×10^{-2} mmol) in [D$_6$]benzene (1 mL) was subject to three freeze/pump/thaw cycles; H_2 was then added to the reaction mixture at room temperature, which resulted in the *in situ* generation of [PtH(μ-H)(FcPPB)]. ^{1}H NMR (600 MHz, [D$_6$]benzene, 25 °C): δ = 8.21 (d, ^3J(H,H) = 7 Hz, 2H; *o*-B*Ph*$_2$ A), 8.09 (dd, ^3J(H,P) = 11 Hz, ^3J(H,H) = 7 Hz, 2H; *o*-P*Ph*$_2$ A), 7.72 (d, ^3J(H,H) = 7 Hz, 1H; C*H*^{6}), 7.61 (d, ^3J(H,H) = 7 Hz, 2H; *o*-B*Ph*$_2$ B), 7.48 (t, ^3J(H,H) = 7 Hz, 2H; *m*-B*Ph*$_2$ A), 7.31 (t, ^3J(H,H) = 7 Hz, 1H; *p*-B*Ph*$_2$ A), 7.29–7.24 (m, 3H; *m*+*p*-B*Ph*$_2$ B), 7.08 (t, ^3J(H,H) = 7 Hz, 1H; C*H*^{5}), 7.04 (t, ^3J(H,H) = 7 Hz, 1H; C*H*^{4}), 7.01–6.95 (m, 6H; *m*+*p*-P*Ph*$_2$ A and B), 6.91 (t, ^3J(H,H) = 7 Hz, 1H; C*H*^{3}), 6.87 (dd, ^3J(H,P) = 13 Hz, ^3J(H,H) = 7 Hz, 2H; *o*-P*Ph*$_2$ B), 4.76 (s, 1H; C*H*$^{2'/5'}$), 4.45 (s, 1H; C*H*$^{2''/5''}$), 4.37 (s, 1H; C*H*$^{5'/2'}$), 3.96 (s, 1H; C*H*$^{3''/4''}$), 3.94 (s, 1H; C*H*$^{3'/4'}$), 3.75 (s, 1H; C*H*$^{4'/3'}$), 3.59 (s, 1H; C*H*$^{4''/3''}$), 3.56 (s, 1H; C*H*$^{5''/2''}$), 1.30 (d, ^3J(H,P) = 14 Hz, 9H; C*Me*$_3$), –2.76 (dd, ^1J(H,Pt) = 792 Hz, ^2J(H,P) = 95 Hz, ^2J(H,P) = 10 Hz, 1H; Pt–*H*–B), –5.19 (ddd, ^1J(H,Pt) = 905 Hz, ^2J(H,P) = 177 Hz, ^2J(H,P) = 24 Hz, ^2J(H,H) = 2 Hz, 1H; Pt–*H*); ^{13}C{^{1}H} NMR (151 MHz, [D$_6$]benzene, 25 °C): δ = 165.0 (broad s; *C*^{2}), 154.6 (broad s; *ipso*-B*Ph*$_2$ A), 148.8 (broad s; *ipso*-B*Ph*$_2$ B), 138.5 (d, ^1J(C,P) = 48 Hz; *C*^{1}), 138.5 (s; *o*-B*Ph*$_2$ B), 136.6 (s; *o*-B*Ph*$_2$ A), 135.8 (d, ^2J(C,P) = 13 Hz; *o*-P*Ph*$_2$ A), 135.8 (d, ^1J(C,P) = 60 Hz; *ipso*-P*Ph*$_2$ A), 135.0 (d, ^2J(C,P) = 18 Hz; *C*^{6}), 134.1 (d, ^1J(C,P) = 60 Hz; *ipso*-P*Ph*$_2$ B), 133.6 (d, ^2J(C,P) = 14 Hz; *o*-P*Ph*$_2$ B), 132.5 (s; *C*^{4}), 131.2 (s; *p*-P*Ph*$_2$ A), 130.4 (s; *C*^{5}), 130.1 (s; *p*-P*Ph*$_2$ B), 128.1 (d, ^3J(C,P) = 11 Hz; *m*-P*Ph*$_2$ A), 127.8 (d, ^3J(C,P) = 12 Hz; *m*-P*Ph*$_2$ B), 127.6 (s; *m*-B*Ph*$_2$ A), 127.1 (s; *m*-B*Ph*$_2$ B), 125.7 (s; *p*-B*Ph*$_2$ A and B), 124.9 (d, ^3J(C,P) = 6 Hz; *C*^{3}), 88.3 (dd, ^1J(C,P) = 58 Hz, ^3J(C,P) = 7 Hz; *C*$^{1''}$), 80.7 (d, ^1J(C,P) = 40 Hz; *C*$^{1'}$), 77.1 (d, ^3J(C,P) = 10 Hz; *C*$^{5''/2''}$), 75.0 (d, ^3J(C,P) = 10 Hz; *C*$^{2''/5''}$), 74.8 (s; *C*$^{2'/5'}$), 74.7 (s; *C*$^{5'/2'}$), 73.3 (d, ^2J(C,P) = 8 Hz; *C*$^{3'/4'}$), 70.4 (d, ^2J(C,P) = 6 Hz; *C*$^{3''/4''}$), 69.6 (s; *C*$^{4'/3'}$), 68.7 (d, ^2J(C,P) = 6 Hz; *C*$^{4''/3''}$), 35.0 (d, ^1J(C,P) = 30 Hz; *C*Me$_3$), 29.7 (d, ^2J(C,P) = 5 Hz; C*Me*$_3$); ^{31}P{^{1}H} NMR (242 MHz, [D$_6$]benzene, 25 °C): δ = 64.3 (dd, ^1J(P,Pt) = 2123 Hz, ^2J(P,H) = 19 Hz, ^2J(P,P) = 10 Hz; C$_5$H$_4$*P*(^{t}Bu)Ar), 24.1 (d, ^1J(Pt,P) = 3721 Hz, ^2J(P,P) 10 Hz; C$_5$H$_4$*P*Ph$_2$); ^{11}B NMR (161 MHz, [D$_6$]benzene, 25 °C): δ = 6 (broad s, $\omega_{1/2}$ = 1200 Hz); ^{11}B NMR (161 MHz, [D$_2$]methylene chloride, 25 °C): δ = 5 (broad s, $\omega_{1/2}$ = 1200 Hz); ^{195}Pt{^{1}H} NMR (128 MHz, [D$_2$]methylene chloride, 25 °C): δ –4980 (dd, ^1J(Pt,P) = 3753 Hz, ^1J(Pt,P) = 2130 Hz); IR (CH_2Cl_2)**:** ν = 2020 cm^{-1} (Pt–H, br), 1822 cm^{-1} (Pt–H–B, ν. br). Elemental analysis could not be obtained due to the instability of **4** under dynamic vacuum.

[PtD(μ-D)(FcPPB)] (4-D): This compound was generated by the same method as described for compound **4**, however using D_2 instead of H_2. IR (CH_2Cl_2): ν = 1478 cm^{-1} (Pt–D, br). The Pt–D–B stretch was not located due to broadness combined with spectral overlap [predicted 1428 cm^{-1} (Pt–D) and 1288 cm^{-1} (Pt–D–B) by Hooke's Law].

Spectroscopic data for [Pt(C$_2$Ph)(μ-H)(FcPPB)] (5): NMR data was collected via *in situ* generation of compound **5**; IR data was collected following evaporation of the reaction solvent *in vacuo*, thus isolating a sample that contained compounds **5** and **6A** in an approximate 1:1 ratio. The IR data was collected in nujol. ^{1}H NMR (500 MHz, [D$_6$]benzene, 25 °C): δ = 8.40 (q, ^3J(H,P) = 11 Hz, ^3J(H,H) = 8 Hz, 2H; phenyl-C*H*), 7.80 (d, ^3J(H,H) = 7 Hz, 2H; phenyl-C*H*), 7.75 (d, ^3J(H,H) = 7 Hz, 1H; phenyl-C*H*), 7.53–7.49 (m, 3H; phenyl-C*H*), 7.34–7.30 (m, 5 H; phenyl-C*H*), 7.01–6.96 (m, 6H; phenyl-C*H*), 6.85–6.84 (m, 4H; phenyl-C*H*), 4.88 (s, 1H; C$_5$*H*$_4$), 4.33 (s, 1H; C$_5$*H*$_4$), 4.27 (s, 1H; C$_5$*H*$_4$), 3.96 (s, 1H; C$_5$*H*$_4$), 3.85 (s, 1H; C$_5$*H*$_4$), 3.76 (s, 1H; C$_5$*H*$_4$), 3.71 (s, 1H; C$_5$*H*$_4$), 3.55 (s, 1H; C$_5$*H*$_4$), 1.29 (d, ^3J(H,P) = 15 Hz, 9H; C*Me*$_3$), –3.69 (dd, ^1J(H,Pt) = 760 Hz, ^2J(H,P) = 115 Hz, ^2J(H,P) **=** 12 Hz, 1H; Pt(μ-*H*)); ^{31}P{^{1}H} NMR (203 MHz, [D$_6$]benzene, 25 °C): δ = 62.9 (d, ^1J(P,Pt) = 2594 Hz, ^2J(P,P) 12 Hz; C$_5$H$_4$*P*(^{t}Bu)Ar), 27.8 (d, ^1J(Pt,P) = 3252 Hz, ^2J(P,P) 12 Hz; C$_5$H$_4$*P*Ph$_2$); ^{11}B NMR (161

MHz, [D_6]benzene, 25 °C): δ = 11 (broad s, $\omega_{1/2}$ = 1500 Hz); IR (nujol)**:** ν = 2126 cm^{-1} (C≡C).

***cis*-[Pt(FcPPB')] (6A/6B):** A solution of [Pt(FcPPB)] · 0.3hexanes (78.9 mg, 8.58×10^{-2} mmol) and PhC_2H (9.0 mg, 8.81×10^{-2} mmol) in benzene (10 mL) was allowed to stir for 6 days at room temperature. The reaction mixture was then evaporated to dryness *in vacuo* to yield a yellow/brown oily residue. Hexanes (20 mL) were added to the crude product and the resulting solution was sonicated for 15 minutes, after which point the resulting solution was evaporated to dryness *in vacuo* to yield a beige solid, which consisted of **6A** and **6B** in a 45:55 ratio. Yield = 65 mg (76 %). Single crystals of **6A** were obtained by dissolving a mixture of **6A** and **6B** in benzene/hexanes and cooling to –30 °C. **NMR data for 6A**: ^{1}H NMR (600 MHz, [D_6]benzene, 25 °C): δ = 8.32 (d, ^3J(H,H) = 8 Hz, 2H; *o*-B*Ph*), 8.11 (dd, ^3J(H,P) = 11 Hz, ^3J(H,H) = 8 Hz, 2H; *o*-PPh_2 A), 7.72 (d, ^3J(H,H) = 8 Hz, 1H; CH^6), 7.51 (t, ^3J(H,H) = 8 Hz, 2H; *m*-B*Ph*), 7.32 (t, ^3J(H,H) = 7 Hz, 1H; *p*-B*Ph*), 7.22 (dd, ^3J(H,P) = 11 Hz, ^3J(H,H) = 8 Hz, 2H; *o*-PPh_2 B), 7.14 (d, ^3J(H,H) = 8 Hz, 2H; *o*-Ph^{α}), 7.08–7.03 (m, 3H; *m*-PPh_2 A, CH^5), 6.98 (dt, ^3J(H,H) = 7 Hz, ^5J(H,P) = 1 Hz, 1H; *p*-PPh_2 A), 6.91–6.87 (m, 6H; *m*+*p*-Ph^{α}, *o*-Ph^{β}, CH^4), 6.78 (t, ^3J(H,H) = 7 Hz, 1H; CH^3), 6.63 (dt, ^3J(H,H) = 7 Hz, ^5J(H,P) = 1 Hz, 1H; *p*-PPh_2 B), 6.60–6.56 (m, 3H; *m*+*p*-Ph^{β}), 6.54 (dt, ^3J(H,H) = 8 Hz, ^4J(H,P) = 2 Hz, 2H; *m*-PPh_2 B), 5.86 (dd, ^2J(H,Pt) = 46 Hz, ^3J(H,P) = 10 Hz, ^3J(H,P) = 5 Hz, 1H; vinylC$^{\beta}$–*H*), 4.99 (s, 1H; C$H^{2'/5'}$), 4.65 (s, 1H; C$H^{2''/5''}$), 4.45 (s, 1H; C$H^{5'/2'}$), 4.43 (s, 1H; C$H^{5''/2''}$), 4.05 (s, 1H; C$H^{3'/4'}$), 4.04 (s, 1H; C$H^{4''/3''}$), 4.03 (s, 1H; C$H^{3''/4''}$), 3.91 (s, 1H; C$H^{4'/3'}$), 0.97 (d, ^3J(H,P) = 15 Hz, 9H; CMe_3); ^{13}C{^{1}H} NMR (151 MHz, [D_6]benzene, 25 °C): δ = 165.7 (broad s; C^2), 151.4 (broad s; *ipso*-B*Ph*), 147.4 (d, ^1J(C,P) = 46 Hz; C^1), 145.9 (d, ^3J(C,P) = 3 Hz; *ipso*-Ph^{α}), 142.7 (s; *ipso*-Ph^{β}), 138.6 (d, ^1J(C,P) = 44 Hz; *ipso*-PPh_2 A), 135.6 (d, ^2J(C,P) = 15 Hz; *o*-PPh_2 A), 134.6 (appt. d, *J* = 27 Hz; *ipso*-PPh_2 B, C^6), 134.2 (s; *o*-B*Ph*), 132.7 (s; *p*-Ph^{α}), 131.5 (s; *o*-Ph^{β}), 131.4 (d, ^2J(C,P) = 13 Hz; *o*-PPh_2 B), 130.6 (s; *p*-PPh_2 A, *o*-Ph^{α}), 129.7 (s; C^5), 128.4 (s; *o*-Ph^{α}), 128.3 (d, ^3J(C,P) = 11 Hz; *m*-PPh_2 A), 128.2 (s; *p*-PPh_2 B), 127.6 (d, ^3J(C,P) = 10 Hz; *m*-PPh_2 B), 127.3 (s; *m*-B*Ph*), 126.7 (s; *m*-Ph^{β}), 126.6 (s; *m*-Ph^{α}), 125.7 (s; *p*-B*Ph*), 124.7 (d, ^4J(C,P) = 6 Hz; C^4), 124.3 (s; *p*-Ph^{β}), 123.7 (s; C^3), 114.0 (broad s; vinylC$^{\alpha}$), 85.9 (d, ^1J(C,P) = 51 Hz; $C^{1''}$), 82.4 (d, ^1J(C,P) = 40 Hz; $C^{1'}$), 77.7 (dd, ^2J(C,P) = 34 Hz, ^2J(C,P) = 4 Hz; vinylC$^{\beta}$), 75.0 (d, ^2J(C,P) = 13 Hz; $C^{2'/5'}$), 74.6 (d, ^2J(C,P) = 6 Hz; $C^{5'/2'}$), 74.5 (s; $C^{2''/5''}$), 73.7 (s; $C^{5''/2''}$), 71.7 (d, ^3J(C,P) = 6 Hz; $C^{3'/4'}$), 70.2 (d, ^3J(C,P) = 7 Hz; $C^{3''/4''}$), 69.7 (s; $C^{4'/3'}$), 69.2 (s; $C^{4''/3''}$), 35.5 (d, ^1J(C,P) = 24 Hz; *C*Me$_3$), 29.1 (d, ^2J(C,P) = 5 Hz, CMe_3); ^{31}P{^{1}H} NMR (203 MHz, [D_6]benzene, 25 °C): δ = 50.3 (d, ^1J(P,Pt) = 3695 Hz, ^2J(P,P) 19 Hz; $C_5H_4P(^t$Bu)Ar), 27.6 (d, ^1J(Pt,P) = 3937 Hz, ^2J(P,P) 19 Hz; C_5H_4PPh$_2$); ^{11}B NMR (161 MHz, [D_6]benzene, 25 °C): δ = 24 (broad s, $\omega_{1/2}$ = 1200 Hz); ^{11}B NMR (161 MHz, [D_2]methylene chloride, 25 °C): δ = 24 (broad s, $\omega_{1/2}$ = 1200 Hz); ^{195}Pt{^{1}H} NMR (128 MHz, [D_2]methylene chloride, 25 °C): *δ* –5117 (dd, ^1J(Pt,P) = 3950 Hz, ^1J(Pt,P) = 3689 Hz). **NMR Data for (6B):** ^{1}H NMR (500 MHz, [D_6]benzene, 25 °C): δ = 7.88 (dq, ^3J(H,P) = 11 Hz, ^3J(H,H) = 8 Hz, ^4J(H,H) = 2 Hz, 2H; *o*-PPh_2 A or B), 7.84 (d, ^3J(H,H) = 7 Hz, 2H; *o*-B*Ph*), 7.73–7.70 (m, 3H; *o*-Ph^{α}, phenyl-C*H*), 7.28–7.21 (m, 4H; phenyl-C*H*), 7.14–6.96 (m, 11H; phenyl-C*H*), 6.85–6.84 (m, 5H; phenyl-C*H*), 6.81–6.75 (m, 2H; phenyl-C*H*), 5.20 (dd, ^2J(H,Pt) = 55 Hz, ^3J(H,P) = 15 Hz, ^3J(H,P) = 5 Hz, 1H; vinylC$^{\beta}$-*H*), 4.88 (s, 1H; C_5H_4), 4.41 (s, 1H; C_5H_4), 4.23 (s, 1H; C_5H_4), 4.18 (s, 1H; C_5H_4), 3.95 (s, 1H; C_5H_4), 3.91 (s, 1H; C_5H_4), 3.84 (s, 1H; C_5H_4), 3.81 (s, 1H; C_5H_4), 1.01 (d, ^3J(H,P) = 15 Hz, 9H; CMe_3); ^{13}C{^{1}H} NMR (151 MHz, [D_6]benzene, 25 °C):

δ = 162.9 (broad s; phenyl-*C*), 152.1 (broad s; *ipso*-B*Ph*), 147.5 (d, ^1J(C,P) = 47 Hz; *ipso*-phenyl-*C*), 145.5 (dd, ^1J(C,P) = 45 Hz, *J*(C,P) = 9 Hz; phenyl-*C*), 144.1 (d, *J*(C,P) = 6 Hz; phenyl-*C*), 143.8 (d, *J*(C,P) = 4 Hz, phenyl-*C*), 138.6 (d, ^1J(C,P) = 42 Hz; *ipso*-phenyl-*C*), 137.2 (d, *J*(C,P) = 17 Hz; *o*-PPh_2 A or B), 135.8 (d, *J*(C,P) = 24 Hz; phenyl-*C*), 135.6 (s; *o*-B*Ph*), 134.0 (d, ^1J(C,P) = 39 Hz; phenyl-*C*), 133.5 (d, ^3J(C,Pt) = 24 Hz, ^4J(C,P) = 4 Hz; *o*-Ph^{α}), 133.1 (s, phenyl-*C*), 132.6 (d, *J*(C,P) = 6 Hz; phenyl-*C*), 132.0 (d, *J*(C,P) = 13 Hz; phenyl-*C*), 131.2 (s; phenyl-*C*), 130.2 (s; phenyl-*C*), 129.2 (s; phenyl-*C*), 128.3 (s; phenyl-*C*), 128.0 (d, *J*(C,P) = 10 Hz; phenyl-*C*), 127.4 (s; phenyl-*C*), 127.1 (s; phenyl-*C*), 126.8 (s; phenyl-*C*), 125.4 (s; phenyl-*C*), 125.2 (d, *J*(C,P) = 6 Hz; phenyl-*C*), 124.4 (s; phenyl-*C*), 93.8 (broad s; vinylC^{α}), 89.5 (dd, ^1J(C,P) = 51 Hz, ^3J(C,P) = 4 Hz, $C^{1''}$), 85 5 (d, ^1J(C,P) = 36 Hz; $C^{1'}$), 75.7 (d, *J*(C,P) = 12 Hz; C_5H_4), 74.5 (d, *J*(C,P) = 13 Hz; C_5H_4), 74.1 (d, *J*(C,P) = 7 Hz; C_5H_4), 73.7 (d, *J*(C,P) = 3 Hz; C_5H_4), 73.1 (d, *J*(C,P) = 4 Hz; C_5H_4), 71.6 (dd, ^2J(C,P) = 37 Hz, ^2J(C,P) = 5 Hz; vinylC^{β}), 71.3 (d, *J*(C,P) = 7 Hz; C_5H_4), 69.9 (d, *J*(C,P) = 3 Hz; C_5H_4), 69.7 (s; C_5H_4), 69.2 (d, *J*(C,P) = 4 Hz; C_5H_4), 35.2 (d, ^1J(C,P) = 66 Hz; *C*Me$_3$), 30.3 (d, ^2J(C,P) = 7 Hz, CMe_3); ^{31}P{^{1}H} NMR (203 MHz, [D_6]benzene, 25 °C): δ = 55.7 (d, ^1J(P,Pt) = 3449 Hz, ^2J(P,P) 20 Hz; $C_5H_4P(^t$Bu)Ar), 23.3 (d, ^1J(Pt,P) = 4090 Hz, ^2J(P,P) 20 Hz; C_5H_4PPh$_2$); ^{11}B NMR (161 MHz, [D_6]benzene, 25 °C): δ = 32 (broad s, $\omega_{1/2}$ = 1500 Hz); ^{11}B NMR (161 MHz, [D_2]methylene chloride, 25 °C): δ = 30 (broad s, $\omega_{1/2}$ = 1500 Hz); ^{195}Pt{^{1}H} NMR (128 MHz, [D_2]methylene chloride, 25 °C): *δ* –4840 (dd, ^1J(Pt,P) = 4097 Hz, ^1J(Pt,P) = 3440 Hz). Elemental analysis calcd (%) for $C_{52}H_{47}BFeNP_2Pt$ (**6A/6B**): C 62.73; H 4.76; found: C 62.48, H 4.73.

[D_5]*cis*-[Pt(FcPPB')] (6A/6B-D): This compound was generated by the same method as described for compounds **6A/6B**, however using $HC_2(C_6D_5)$ instead of $HC_2(C_6H_5)$. The NMR spectra were identical to that of a mixture of **6A/6B**, however with the C_6H_5 resonances from the activated HC_2Ph unit missing from the ^{1}H and ^{13}C NMR spectra.

DFT Calculations: All structures were fully optimized with the ADF DFT package (SCM, version 2013.01).[51] Calculations were conducted using the zero-order regular approximation (ZORA)[52] for relativistic effects, and 1996 Perdew-Burke-Ernzerhof exchange and correlation for the GGA part of the density functional (PBE),[53] combined with Grimme's DFT-D3-BJ dispersion correction.[54] All calculations were restricted gas-phase calculations. Preliminary geometry optimizations were conducted with frozen cores corresponding to the configuration of the preceding noble gas (core = medium) using a double-ζ basis set with one polarization function (DZP), an integration value of 5, and default convergence criteria. These structures were further refined using an all-electron TZ2P basis set (the size and quality of ADF basis sets increases in the order SZ < DZ < DZP < TZP < TZ2P < QZ4P) and an integration value of 7. Analytical frequency calculations for all complexes showed no imaginary frequencies. Visualization of the computational results was performed using the ADF-GUI (SCM) or Discovery Studio Visualizer (Accelrys).

Table 1. Crystallographic Data Collection and Refinement Parameters for FcPPB and Compounds 1–3 and 6A.

Compound	FcPPB	1·CH_2Cl_2	2·2CH_2Cl_2	3·CH_2Cl_2	6A·4C_6H_6
Formula	$C_{44}H_{41}BFeP_2$	$C_{44}H_{41}BFeP_2Pt$ ·CH_2Cl_2	$C_{45}H_{41}BFeOP_2Pt$ ·2CH_2Cl_2	$C_{106}H_{100}B_2Fe_2N_2P_4Pt_2$ ·2CH_2Cl_2	$C_{52}H_{47}BFeP_2Pt$ ·4C_6H_6
Formula wt [g mol^{-1}]	698.37	978.38	1091.32	2219.11	1308.02
T [K]	100(2)	100(2)	100(2)	100(2)	100(2)
Cryst. Syst.	Triclinic	Triclinic	Triclinic	Monoclinic	Monoclinic
Space Group	*P*$\bar{1}$	*P*$\bar{1}$	*P*$\bar{1}$	*Cc*	$P2_1/n$
a [Å]	9.0532(8)	10.787(2)	9.897(1)	21.645(3)	17.313(3)
b [Å]	10.3272(9)	13.260(2)	11.960(2)	12.0075(16)	19.108(3)
c [Å]	19.361(2)	14.740(3)	19.840(3)	35.074(5)	19.095(3)
α [deg]	101.061(2)	71.759(4)	101.204(3)	90	90
β [deg]	91.972(2)	77.594(3)	92.005(2)	94.283(3)	104.823(2)
γ [deg]	102.617(2)	83.677(3)	109.936(2)	90	90
Volume [$Å^3$]	1728.1(3)	1953.5(6)	2152.5(5)	9090(2)	6107(2)
Z	2	2	2	4	4
Density [calcd; mg/m^3]	1.342	1.663	1.684	1.621	1.423
μ [mm^{-1}]	0.561	4.199	3.942	3.621	2.622
F(000)	732	972	1084	4448	2664
Crystal Size [mm^3]	0.22×0.10×0.08	0.26×0.12×0.04	0.21×0.14×0.08	0.19×0.16×0.09	0.17×0.08×0.04
θ Range for Collection [deg]	1.08–28.33	1.48–31.62	1.05–26.29	1.89–26.45	1.62–26.66
No. of reflns collected	33862	27043	23370	51591	82018
No. of indep reflns	8547	12749	8557	11518	12677
Completeness to θ Max [%]	99.3	97.1	98.1	99.8	98.6
Absorption Correction	Numerical	Numerical	Numerical	Numerical	Numerical
Max and Min Transmission	0.9565, 0.8865	0.8500, 0.4081	0.7433, 0.4915	0.7364, 0.5462	0.9024, 0.6641
GOF on F^2	1.086	1.004	1.034	1.043	1.063
Final R_1 [$I > 2\sigma(I)$] [%]	3.52	3.45	3.47	4.00	4.60
CCDC no.	1019205	1019206	1019207	1019208	1019209

Acknowledgements

D.J.H.E. thanks NSERC of Canada for a Discovery Grant and B.E.C. thanks the Government of Canada for an NSERC PGS-D scholarship.

Keywords: Boranes • Phosphane ligands • Ligand design • Donor-acceptor systems • Coordination modes

[1] W. H. Harman, T.-P. Lin, J. C. Peters, *Angew. Chem.* **2014,** *126,* 1099-1104; *Angew. Chem. Int. Ed.* **2014**, *53*, 1081-1086.

[2] T.-P. Lin, R. C. Nelson, T. Wu, J. T. Miller, F. Gabbaï, *Chem. Sci.* **2012**, *3*, 1128-1136.

[3] G. Parkin, *Organometallics* **2006**, *25*, 4744-4747.

[4] M. Sircoglou, S. Bontemps, M. Mercy, N. Saffon, M. Takahashi, G. Bouhadir, L. Maron, D. Bourissou, *Angew. Chem.* **2007,** *119,* 8737-8740; *Angew. Chem. Int. Ed.* **2007**, *46*, 8583-8586.

[5] A. Amgoune, D. Bourissou, *Chem. Commun.* **2011**, *47*, 859-871.

[6] M.-E. Moret, J. C. Peters, *Angew. Chem.* **2011,** *123,* 2111-2115; *Angew. Chem. Int. Ed.* **2011**, *50*, 2063-2067.

[7] S. Bontemps, G. Bouhadir, K. Miqueu, D. Bourissou, *J. Am. Chem. Soc.* **2006**, *128*, 12056-12057.

[8] a) J. Vergnaud, T. Ayed, K. Hussein, L. Vendier, M. Grellier, G. Bouhadir, J.-C. Barthelat, S. Sabo-Etienne, D. Bourissou, *Dalton Trans.* **2007**, 2370-2372; b) S. Bontemps, G. Bouhadir, D. C. Aperley, P. W. Dyer, K. Miqueu, D. Bourissou, *Chem. Asian J.* **2009**, *4*, 428-435.

[9] a) K. Pang, J. M. Tanski, G. Parkin, *Chem. Commun.* **2008**, 1008-1010; b) J. S. Figueroa, J. G. Melnick, G. Parkin, *Inorg. Chem.* **2006**, *45*, 7056-7058; c) I. R. Crossley, A. F. Hill, *Dalton Trans.* **2008**, 201-203; d) L. Turculet, J. D. Feldman, T. D. Tilley, *Organometallics* **2004**, *23*, 2488-2502; e) A. Fischbach, P. R.

Bazinet, R. Waterman, T. D. Tilley, *Organometallics* **2008**, *27*, 1135-1139; f) E. Khaskin, P. Y. Zavalij, A. N. Vedernikov, *J. Am. Chem. Soc.* **2008**, *130*, 10088-10089; g) S. Fromel, G. Kehr, R. Frohlich, C. G. Daniliuc, G. Erker, *Dalton Trans.* **2013**, *42*, 14531-14536; h) S. Pal, A. N. Vedernikov, *Dalton Trans.* **2012**, *41*, 8116-8122; (i) E. Khaskin, P. Y. Zavalij, A. N. Vedernikov, *Angew. Chem.* **2007,** *119,* 6425-6428; *Angew. Chem. Int. Ed.* **2007**, *46*, 6309-6312; j) S. K. Podiyanachari, R. Fröhlich, C. G. Daniliuc, J. L. Petersen, C. Mück-Lichtenfeld, G. Kehr, G. Erker, *Angew. Chem.* **2012,** *124,* 8960-8963; *Angew. Chem. Int. Ed.* **2012**, *51*, 8830-8833; k) S. K. Podiyanachari, G. Kehr, C. Mück-Lichtenfeld, C. G. Daniliuc, G. Erker, *J. Am. Chem. Soc.* **2013**, *135*, 17444-17456; l) J. Zhu, D. Mukherjee, A. D. Sadow, *Chem. Commun.* **2012**, *48*, 464-466; m) J. F. Dunne, K. Manna, J. W. Wiench, A. Ellern, M. Pruski, A. D. Sadow, *Dalton Trans.* **2010**, *39*, 641-653.

[10] D. J. H. Emslie, J. M. Blackwell, J. F. Britten, L. E. Harrington, *Organometallics* **2006**, *25*, 2412-2414.

[11] B. E. Cowie, D. J. H. Emslie, H. A. Jenkins, J. F. Britten, *Inorg. Chem.* **2010**, *49*, 4060-4072.

[12] H. Fong, M.-E. Moret, L. Yunho, J. C. Peters, *Organometallics* **2013**, *32*, 3053-3062.

[13] a) I. R. Crossley, A. F. Hill, A. C. Willis, *Organometallics* **2007**, *26*, 3891-3895; b) A. J. M. Miller, J. A. Labinger, J. E. Bercaw, *Organometallics* **2011**, *30*, 4308-4314; c) A. J. M. Miller, J. A. Labinger, J. E. Bercaw, *Organometallics* **2010**, *29*, 4499-4516; d) A. J. M. Miller, J. A. Labinger, J. E. Bercaw, *J. Am. Chem. Soc.* **2008**, *130*, 11874-11875.

[14] W. H. Harman, J. C. Peters, *J. Am. Chem. Soc.* **2012**, *134*, 5080-5082.

[15] S. N. MacMillan, W. H. Harman, J. C. Peters, *Chem. Sci.* **2014**, *5*, 590-597.

[16] R. Malacea, N. Saffon, M. Gómez, D. Bourissou, *Chem. Commun.* **2011**, *47*, 8163-8165.

[17] A. F. Hill, G. R. Owen, A. J. P. White, D. J. Williams, *Angew. Chem.* **1999,** *38,* 2759-2761; *Angew. Chem. Int. Ed.* **1999**, *38*, 2759-2761.

[18] a) M. Sircoglou, S. Bontemps, G. Bouhadir, N. Saffon, K. Miqueu, W. Gu, M. Mercy, C.-H. Chen, B. M. Foxman, L. Maron, O. V. Ozerov, D. Bourissou, *J. Am. Chem. Soc.* **2008**, *130*, 16729-16738; b) S. Bontemps, M. Sircoglou, G. Bouhadir, H. Puschmann, J. A. K. Howard, P. W. Dyer, K. Miqueu, D. Bourissou, *Chem. Eur. J.* **2008**, *14*, 731-740; c) G. Bouhadir, A. Amgoune, D. Bourissou, *Adv. Organomet. Chem.* **2010**, *58*, 1-107.

[19] a) M.-E. Moret, J. C. Peters, *J. Am. Chem. Soc.* **2011**, *133*, 18118-18121; b) D. L. M. Suess, C. Tsay, J. C. Peters, *J. Am. Chem. Soc.* **2012**, *134*, 14158-14164; c) J. S. Anderson, M.-E. Moret, J. C. Peters, *J. Am. Chem. Soc.* **2013**, *135*, 534-537; d) M.-E. Moret, L. Zhang, J. C. Peters, *J. Am. Chem. Soc.* **2013**, *135*, 3792-3795; e) D. L. M. Suess, J. C. Peters, *J. Am. Chem. Soc.* **2013**, *135*, 12580-12583; f) D. L. M. Suess, J. C. Peters, *J. Am. Chem. Soc.* **2013**, *135*, 4938-4941.

[20] H. Kameo, Y. Hashimoto, H. Nakazawa, *Organometallics* **2012**, *31*, 3155-3162.

[21] H. Kameo, H. Nakazawa, *Organometallics* **2012**, *31*, 7476-7484.

[22] a) M. P. Boone, D. W. Stephan, *J. Am. Chem. Soc.* **2013**, *135*, 8508-8511; b) M. P. Boone, D. W. Stephan, *Chem. Eur. J.* **2014**, *20*, 3333-3341.

[23] E. S. Smirnova, A. M. Echavarren, *Angew. Chem.* **2013,** *125,* 9193-9196; *Angew. Chem. Int. Ed.* **2013**, *52*, 9023-9026.

[24] M. Sircoglou, S. Bontemps, M. Mercy, K. Miqueu, S. Ladeira, N. Saffon, L. Maron, G. Bouhadir, D. Bourissou, *Inorg. Chem.* **2010**, *2010*, 3983-3990.

[25] S. R. Oakley, K. D. Parker, D. J. H. Emslie, I. Vargas-Baca, C. M. Robertson, L. E. Harrington, J. F. Britten, *Organometallics* **2006**, *25*, 5835-5837.

[26] D. J. H. Emslie, L. E. Harrington, H. A. Jenkins, C. M. Robertson, J. F. Britten, *Organometallics* **2008**, *27*, 5317-5325.

[27] B. E. Cowie, D. J. H. Emslie, *Organometallics* **2013**, *32*, 7297-7305.

[28] D. J. H. Emslie, B. E. Cowie, S. R. Oakley, N. L. Huk, H. A. Jenkins, L. E. Harrington, J. F. Britten, *Dalton Trans.* **2012**, *41*, 3523-3535.

[29] a) A. Fihri, P. Meunier, J.-C. Hierso, *Coord. Chem. Rev.* **2007**, *251*, 2017-2055; b) S. W. Chien, T. S. A. Hor, in *Ferrocenes: Ligands, Materials and Biomolecules* (Ed.: P. Štěpnička), John Wiley and Sons Ltd, West Sussex, England, **2008**, pp. 33-116; c) K. S. Gan, T. S. A. Hor, in *Ferrocenes: Homogenous Catalysis, Organic Synthesis, Materials Science* (Eds.: A. Togni, T. Hayashi), VCH, Weinheim, Germany, **1995**, pp. 3-104.

[30] I. R. Butler, R. L. Davies, *Synthesis* **1996**, 1350-1354.

[31] S. Bontemps, G. Bouhadir, P. W. Dyer, K. Miqueu, D. Bourissou, *Inorg. Chem.* **2007**, *46*, 5149-5151.

[32] H. C. Brown, U. S. Racherla, *J. Org. Chem.* **1986**, *51*, 427-432.

[33] B. Crociani, F. Benetollo, R. Bertani, G. Bombieri, F. Meneghetti, L. Zanotto, *J. Organomet. Chem.* **2000**, *605*, 28-38.

[34] a) D. Astruc, in *Organometallic Chemistry and Catalysis*, Springer, New York, **2007**, pp. 151-173; b) L. Carlton, L. V. Mokoena, M. A. Fernandes, *Inorg. Chem.* **2008**, *47*, 8696-8703; c) Y. Misumi, H. Seino, Y. Mizobe, *J. Organomet. Chem.* **2006**, *691*, 3157-3164; d) I. R. Crossley, A. F. Hill, E. R. Humphrey, M. K. Smith, *Organometallics* **2006**, *25*, 2242-2247; e) W. W. Brennessel, J. E. Ellis, *Angew. Chem.* **2007,** *119,* 604-606; *Angew. Chem. Int. Ed.* **2007**, *46*, 598-600; f) J. Vincente, M. T. Chicote, I. Vincente-Hernández, D. Bautista, *Inorg. Chem.* **2007**, *46*, 8939-8949.

[35] B. Cordero, V. Gómez, A. E. Platero-Prats, M. Revés, J. Echeverría, E. Cremades, F. Barragán, S. Alvarez, *Dalton Trans.* **2008**, 2832-2838.

[36] N. Nakata, T. Ikeda, A. Ishii, *Inorg. Chem.* **2010**, *49*, 8112-8116.

[37] M. Itazaki, Y. Nishihara, K. Osakada, *Organometallics* **2004**, *23*, 1610-1621.

[38] H. Li, J. A. Aquino, D. B. Cordes, F. Hung-Low, W. L. Hase, C. Krempner, *J. Am. Chem. Soc.* **2013**, *135*, 16066-16069.

[39] The Pt-H-B stretch was not located for compound **5**, presumably due to extreme broadness of the peak; the Pt-H-B stretch for compound **4** was extremely broad.

[40] J. R. Berenguer, M. Bernechea, E. Lalinde, *Organometallics* **2007**, *26*, 1161-1172.

[41] K. B. Kolpin, D. J. H. Emslie, *Angew. Chem.* **2010,** *122*, 2776-2779; *Angew. Chem. Int. Ed.* **2010**, *49*, 2716-2719.

[42] R. H. Crabtree, in *The Organometallic Chemistry of the Transition Metals*, Fifth ed., John Wiley & Sons, Inc., Hoboken, New Jersey, **2009**, pp. 128-131.

[43] B. J. Burger, J. E. Bercaw, in *Experimental Organometallic Chemistry - A Practicum in Synthesis and Characterization, Vol. 357*, American Chemical Society, Washington D.C., **1987**, pp. 79-98.

[44] J. J. Eisch, R. B. King, in *Nontransition metal-compounds, Vol. 2* (Ed.: J. J. Eisch), Academic Press, New York, **1981**, pp. 121-155.

[45] B. Punji, J. T. Mague, M. S. Balakrishna, *Inorg. Chem.* **2007**, *46*, 10268-10275.

[46] J. J. Bishop, A. Davison, M. L. Katcher, D. W. Lichtenberg, R. E. Merrill, J. C. Smart, *J. Organomet. Chem.* **1971**, *27*, 241-249.

[47] A. Shafir, M. P. Power, G. D. Whitener, J. Arnold, *Organometallics* **2000**, *19*, 3978-3982.

[48] J. X. McDermott, J. F. White, G. M. Whitesides, *J. Am. Chem. Soc.* **1976**, *98*, 6521-6528.

[49] L. E. Crascall, J. L. Spencer, *Inorg. Synth.* **1990**, *28*, 126-132.

[50] J. L. W. Pohlmann, F. E. Brinckman, *Z. Naturforsch.* **1965**, *20b*, 5-11.

[51] G. Fraenkel, A. Chow, W. R. Winchester, *J. Am. Chem. Soc.* **1990**, *112*, 1382-1386.

[52] a) ADF2010, in *SCM, Theoretical Chemistry*, http://www.scm.com, Vrije Universiteit, Amsterdam, The Netherlands; G. t. Velde, F. M. Bickelhaupt, S. J. A. v. Gisbergen, C. F. Guerra, E. J. Baerends, J. G. Snijders, T. J. Ziegler, *Journal of Computational Chemistry* **2001**, *22*, 931-967; b) C. F. Guerra, J. G. Snijders, G. t. Velde, E. Baerends, *J. Theor. Chem. Acc.* **1998**, *99*, 391-403.

[53] a) E. v. Lenthe, E. J. Baerends, G. J. Snijders, *J. Chem. Phys.* **1994**, *101*, 9783-9792; b) E. v. Lenthe, E. J. Baerends, J. G. Snijders, *J. Chem. Phys.* **1993**, *99*, 4597-4610; c) E. v. Lenthe, A. Ehlers, E. J. Baerends, *J. Chem. Phys.* **1999**, *110*, 8943-8953; d) E. v. Lenthe, R. v. Leeuwen, E. J. Baerends, J. G. Snijders, *Int. J. Quantum Chem.* **1996**, *57*, 281-293; e) E. v. Lenthe, J. G. Snijders, E. J. Baerends, *J. Chem. Phys.* **1996**, *105*, 6505-6516.

[54] J. P. Perdew, K. Burke, M. Ernzerhof, *Phys. Rev. Lett.* **1996**, *77*, 3865-3868.

Entry for the Table of Contents (Please choose one layout)

Layout 2:

FULL PAPER

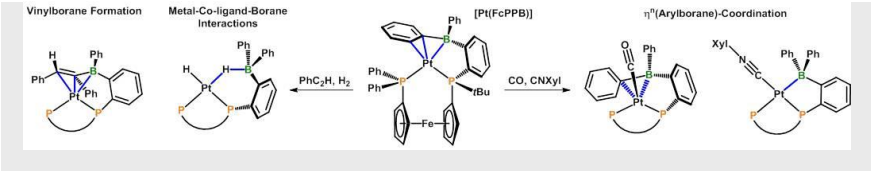

A borane appended analogue of dppf (**FcPPB**) was prepared, and reaction with tris(norbornene)platinum provided [Pt(FcPPB)] in which the arylborane is η^3*BCC*-coordinated. Subsequent reactions of [Pt(FcPPB)] with CO, CNXyl and H_2 afforded complexes featuring η^2*BC*-, η^1*B*- and Pt–H–B coordination modes, respectively. Further, reaction of PhC_2H with [Pt(FcPPB)] afforded [Pt(FcPPB')] in which the arylborane of FcPPB is converted to an η^3*BCC*-coordinated vinylborane.

*Bradley E. Cowie and Prof. David J. H. Emslie**

Page 1 – Page 14

Platinum Complexes of a Borane-Appended Analogue of 1,1'-Bis(diphenylphosphino)ferrocene: Flexible Borane Coordination Modes and *In-Situ* Vinylborane Formation